the plant journal

SEB SOCIETY FOR EXPERIMENTAL BIOLOGY

The Plant Journal (2021) **106,** 1008–1023 doi: 10.1111/tpj.15215

Disentangling cause and consequence: genetic dissection of the *DANGEROUS MIX2* risk locus, and activation of the DM2h NLR in autoimmunity

Jana Ordon[1,†], Patrick Martin[1], Jessica Lee Erickson[1], Filiz Ferik[1,‡], Gerd Balcke[2], Ulla Bonas[1] and Johannes Stuttmann[1,*]

[1]*Institute for Biology, Department of Plant Genetics, Martin Luther University Halle-Wittenberg, Weinbergweg 10, Halle (Saale) 06120, Germany, and*

[2]*Department of Cell and Metabolic Biology, Leibniz Institute of Plant Biochemistry, Weinberg 3, Halle (Saale) 06120, Germany*

Received 2 November 2020; revised 7 February 2021; accepted 22 February 2021; published online 24 February 2021.

*For correspondence (e-mail johannes.stuttmann@genetik.uni-halle.de).

[†]Present address: Department of Plant Microbe Interactions, Max Planck Institute for Plant Breeding Research, Carl-von-Linné-Weg 10, Köln, 50829, Germany

[‡]Present address: Department of Bioengineering, Ege University, Bornova, Izmir, 35040, Turkey

SUMMARY

Nucleotide-binding domain–leucine-rich repeat-type immune receptors (NLRs) protect plants against pathogenic microbes through intracellular detection of effector proteins. However, this comes at a cost, as NLRs can also induce detrimental autoimmunity in genetic interactions with foreign alleles. This may occur when independently evolved genomes are combined in inter- or intraspecific crosses, or when foreign alleles are introduced by mutagenesis or transgenesis. Most autoimmunity-inducing NLRs are encoded within highly variable *NLR* gene clusters with no known immune functions, which were termed autoimmune risk loci. Whether risk NLRs differ from sensor NLRs operating in natural pathogen resistance and how risk NLRs are activated in autoimmunity is unknown. Here, we analyzed the *DANGEROUS MIX2* risk locus, a major autoimmunity hotspot in *Arabidopsis thaliana*. By gene editing and heterologous expression, we show that a single gene, *DM2h*, is necessary and sufficient for autoimmune induction in three independent cases of autoimmunity in accession Landsberg *erecta*. We focus on autoimmunity provoked by an EDS1-yellow fluorescent protein (YFP)^{NLS} fusion protein to characterize DM2h functionally and determine features of EDS1-YFP^{NLS} activating the immune receptor. Our data suggest that risk NLRs function in a manner reminiscent of sensor NLRs, while autoimmunity-inducing properties of EDS1-YFP^{NLS} in this context are unrelated to the protein's functions as an immune regulator. We propose that autoimmunity, at least in some cases, may be caused by spurious, stochastic interactions of foreign alleles with coincidentally matching risk NLRs.

Keywords: plant innate immunity, autoimmunity, hybrid necrosis, EDS1, NLR receptor, TIR domain, SRF3, OASTL-A1, OLD3, CRISPR/Cas, *Arabidopsis thaliana*, *Nicotiana benthamiana*.

INTRODUCTION

Plants growing in natural habitats, as well as crops cultivated in the field, are constantly exposed to pathogenic microbes, which can induce severe damage and yield losses. However, plants evolved two major types of immune receptors to protect from disease (Dodds and Rathjen, 2010; Jones and Dangl, 2006). Extracellularly, membrane-anchored pattern recognition receptors can detect microbe-associated molecular patterns, which induces a suite of responses collectively termed pattern-triggered immunity (PTI; e.g., reviewed in Saijo *et al.*, 2018). Intracellularly, immune receptors belonging to the nucleotide-binding domain–leucine-rich repeat (NLR) class can detect microbial proteins secreted into host cells during the infection process, termed effector proteins, thus inducing effector-triggered immunity (ETI; e.g., reviewed in Cui *et al.*, 2015). Although ETI and PTI are qualitatively similar, they differ in amplitude, and particularly ETI is often accompanied by localized cell death at infection sites – the hypersensitive response (HR). So far, ETI and PTI have largely been considered as independent signaling networks; however, recent reports suggest that plant resistance depends on mutual amplification of PTI and ETI responses (Ngou *et al.*, 2020; Yuan *et al.*, 2020).

Plant NLRs are modular proteins consisting of three domains: a C-terminal leucine-rich repeat (LRR) domain, a central nucleotide-binding (NB-ARC) domain and either a coiled coil (CC) or a Toll/interleukin-1 receptor (TIR) domain at the N-terminus (Bentham *et al.*, 2017; Song *et al.*, 2020). These N-terminal domains initiate immune signaling upon receptor activation, and subdivide plant NLRs into TNLs (TIR domain), CNLs (CC domain) and RNLs, which hold an atypical CC domain with homology to the non-NLR resistance protein RESISTANCE TO POWDERY MILDEW8 (RPW8; Collier *et al.*, 2011; Jubic *et al.*, 2019; Meyers *et al.*, 2003). Structurally similar immune receptors, albeit differing in their N-terminal domains, function in animals and fungi. Activation and signaling by animal NLRs involves oligomerization and interactor recruitment by oligomeric N-terminal assemblies (Bentham *et al.*, 2017). Recent structural elucidation of full-length plant CNL (HOPZ-ACTIVATED RESISTANCE1 [ZAR1]; Wang *et al.*, 2019a, 2019b) and TNL receptors (Recognition of Peronospora parasitica 1 [RPP1]; Ma *et al.*, 2020, Recognition of XopQ1 [Roq1]; Martin *et al.*, 2020b) revealed assembly of pentameric and tetrameric resistosomes by the activated immune receptors, respectively. Resistosome formation is driven by indirect (ZAR1) or direct (Roq1, RPP1) pathogen effector recognition, nucleotide exchange (ADP/ATP) within the nucleotide-binding domain and profound conformational changes. In the ZAR1 resistosome, the N-terminal CC domains assemble into a funnel-like structure, which was proposed to translocate into membranes. Thereby, the ZAR1 resistosome might induce the HR directly by interfering with membrane integrity or by functioning as a selective ion channel (Wang *et al.*, 2019a). In the resistosomes formed by activated Roq1 and RPP1, two dimers of TIR domain dimers exhibit a two-fold symmetry. This conformation leads to opening of the NADase active site of the TIR domain and breakdown of NAD^+ (Duxbury *et al.*, 2020; Horsefield *et al.*, 2019; Ma *et al.*, 2020; Martin *et al.*, 2020b; Wan *et al.*, 2019). In the latter case, it is assumed that one of the breakdown products of the TIR domain enzymatic activity, whose molecular identity remains to be determined, functions as a signaling molecule. In agreement with an indirect mode of action, resistance mediated by TNLs further requires proteins of the ENHANCED DISEASE SUSCEPTIBILITY1 (EDS1) family and RNL-type helper NLRs of the N requirement gene1 (NRG1) and/or the ACTIVATED DISEASE RESISTANCE1 (ADR1) class (Castel *et al.*, 2019; Gantner *et al.*, 2019; Lapin *et al.*, 2019; Saile *et al.*, 2020; Wagner *et al.*, 2013; Wu *et al.*, 2018). Nevertheless, it is unknown how a signal is relayed from activated TNLs to RNLs via EDS1 complexes.

Aside from their beneficial function in conferring resistance to invading pathogens, NLRs may become activated erroneously, thus inducing autoimmunity (Bomblies *et al.*, 2007; Chae *et al.*, 2014). Autoimmune plants exhibit hallmarks of innate immune responses, such as marker gene induction and accumulation of the defense hormone salicylic acid (SA). In addition, plants are commonly dwarfed and exhibit curled leaves, tissue necrosis and spontaneous cell death (Alcazar and Parker, 2011; Bomblies *et al.*, 2007; van Wersch *et al.*, 2016). Autoimmunity has been described in at least three different scenarios: (i) transgenic lines ectopically expressing proteins (e.g., Stuttmann *et al.*, 2016; Xu *et al.*, 2014); (ii) mutant lines obtained in forward genetic screens (e.g., Kim *et al.*, 2010; Li *et al.*, 2001); and (iii) hybrids combining independently evolved alleles, then referred to as hybrid weakness or hybrid incompatibility (HI; Bomblies and Weigel, 2007).

In particular, intraspecific HI has been well-studied in Arabidopsis (*Arabidopsis thaliana*). Different degrees of HI, ranging from mild chlorosis to seedling lethality, occurred in approximately 2% of all hybrids from systematic crossing of accessions representing most of the species' diversity (Bomblies *et al.*, 2007; Chae *et al.*, 2014). Genetic dissection revealed that HI is generally induced by two genetically separable loci at least one of which encodes an NLR (Alcazar *et al.*, 2009; Barragan *et al.*, 2019; Chae *et al.*, 2014). This pinpoints the plant innate immune system as a key player of HI. NLRs identified as causal in Arabidopsis HI include, but are not limited to, numerous *RECOGNITION OF PERONOSPORA PARASITICA* (*RPP*) loci. *RPP* loci were identified as conferring race-specific resistance to different isolates of the obligate biotrophic oomycete *Hyaloperonospora arabidopsidis* (*Hpa*; formerly *Peronospora parasitica*). For example, *RPP2* alleles present in reference accession Columbia (Col), but not those from accession Landsberg *erecta* (L*er*), confer resistance to *Hpa* isolate Cala2 (Sinapidou *et al.*, 2004). Similarly, *RPP5* from accession L*er*, but not genes located at the homologous *RPP4/RPP5* locus in Col, confer resistance to *Hpa* isolate Noco2 (Noël *et al.*, 1999; Parker *et al.*, 1997). In line with the recognition-escape battle ("molecular arms race") dictating natural host–pathogen systems, both *RPP* genes and the corresponding *Hpa* effectors occur in allelic series and are under strong selection (Botella *et al.*, 1998; Rehmany *et al.*, 2005). While gene clustering is rare in eukaryotes, *RPP* genes occur in eventually large and diversified clusters undergoing rapid evolution by conjunction of tandem duplications, illegitimate recombination and gene conversions (Jacob *et al.*, 2013; van Wersch and Li, 2019), thus facilitating functional diversification towards new recognition specificities. Indeed, while NLR-coding genes anyway represent one of the most rapidly evolving gene families in plants, several *RPP* loci stand out as they were identified as particularly prone to variation and rearrangements in Arabidopsis (Jiao and Schneeberger, 2020; Lee and Chae, 2020; Van de Weyer *et al.*, 2019). Altogether, diversified and rapidly evolving NLR loci thus appear particularly prone to induce autoimmunity in intraspecific HI.

The *RPP1* locus, also referred to as *DANGEROUS MIX2* (*DM2*), has been identified as a major hotspot for autoimmunity, and genetically interacts with at least seven distinct loci encoding NLR and non-NLR proteins (Alcazar *et al.*, 2010; Chae *et al.*, 2014; Stuttmann *et al.*, 2016; Tahir *et al.*, 2013). Interestingly, while, e.g., RPP1^{WsB} (from accession Wassilewskija) and RPP1Nd (from accession Niederzenz) confer *Hpa* resistance, beneficial immune functions were not reported for the autoimmunity-inducing "risk alleles" (originating from accessions L*er*, Uk-1, Bla-1, S. Tyrol and Dog 4). The *RPP1/DM2* locus in accession L*er* (*RPP1/DM2*^{Ler}) encodes seven to eight full-length TNLs. Respective genes are referred to as *RPP1-like R1-R8* or *DM2a-DM2h*, with the latter nomenclature utilized hereafter (Alcazar *et al.*, 2009; Chae *et al.*, 2014). *DM2*^{Ler} causes HI when combined with alleles of the receptor kinase *STRUBBELIG-RECEPTOR FAMILY3* (*SRF3*) from the South Asian accessions Kashmir and Kondara (Alcazar *et al.*, 2009, 2010). Furthermore, an EMS-induced allele of an *O*-acetylserine (thiol) lyase (*old3-1*) and ectopic expression of the immune regulator EDS1 in fusion with YFP and a nuclear localization signal (EDS1-YFP^{NLS}) induce autoimmunity in the presence of *DM2*^{Ler} (Stuttmann *et al.*, 2016; Tahir *et al.*, 2013). We previously identified *dm2h* alleles in an EMS screen for genetic suppressors of EDS1-YFP^{NLS}-induced autoimmunity and showed that *DM2h* was also essential for *SRF3*- and *old3-1*-induced autoimmunity (Stuttmann *et al.*, 2016). Until recently, functional studies of risk loci were hampered by the complexity of the respective gene clusters, the similarity between the NLR genes and the strong dosage-dependent effects of transgenic expression of single NLRs. Therefore, the contribution of risk loci to natural pathogen resistance and synergistic and/or epistatic interactions between risk locus-encoded NLRs are still largely unexplored. In addition, the molecular mechanisms underlying autoimmune induction are unknown.

To explore the contribution of risk NLRs to pathogen resistance and autoimmunity and to reveal mechanisms of risk NLR activation, we genetically dissected the *DM2*^{Ler} cluster and reconstituted activation of a *DM2* risk NLR in heterologous expression assays. Relying on unique combinations of *DM2* genes generated by genome editing in the background of the native L*er* accession, we show that the single DM2h immune receptor is necessary and sufficient in all three cases of autoimmunity induced by EDS1-YFP^{NLS}, *old3-1* and *SRF3*. However, we failed to uncover any relevance of the *DM2*^{Ler}-encoded TNLs for resistance to model pathogens. In addition, we functionally evaluated activation of a risk allele by an inducer, EDS1-YFP^{NLS}, in *Nicotiana benthamiana* (*Nb*) agroinfiltration assays and in stable transgenic Arabidopsis. Our data suggest that activation of DM2h occurs by similar mechanisms as for classical sensor NLRs. Intriguingly, we provide evidence that the capacity to activate the NLR and to trigger autoimmunity is unrelated to the physiological activity of the inducer (here, EDS1/EDS1-YFP^{NLS}). Therefore, we propose that autoimmune induction, at least in some cases, may rely on stochastic interactions of a non-native protein with an immune receptor. This emphasizes the importance of exercising caution when drawing conclusions regarding the immune function of a protein based on its ability to trigger an autoimmune response.

RESULTS

Analysis of *nde*-type suppressor mutants: *DM2h* is the main locus required for autoimmunity induced by an EDS1-YFP^{NLS} fusion

Our screen for genetic suppressors of EDS1-YFP^{NLS}-induced autoimmunity previously identified approximately 55 *near death experience* (*nde*) mutant lines (Stuttmann *et al.*, 2016). To elucidate the genetic requirements of autoimmune induction further, we analyzed the remaining *nde* lines. First, we Sanger-sequenced *DM2h* in 30 selected phenotypically stable *nde* mutant lines. Strikingly, 25 of 30 lines carried independent mutations within *DM2h* (Figure 1a; Table S1). We concluded that *DM2h* was the main gene required for EDS1-YFP^{NLS}-induced autoimmunity targeted in our suppressor screen. The predicted *DM2h* gene model encompasses six exons, and encodes for a canonical TNL-type immune receptor (Figure 1a). TIR and NB-ARC domains are highly homologous among TNLs, and the three *nde* mutations mapping to these domains affected conserved residues (Figure S1). Most *nde* mutations affected residues located to the more divergent LRR domain and the LRR-adjacent C-terminal region (Figure 1a). Interestingly, we identified two nonsense mutations (W1129*, W1133*) that truncate DM2h by approximately 40 amino acids.

From the remaining five *nde* lines harboring wild-type *DM2h*, we focused on *nde2*. By a combination of mapping-by-sequencing (using SHORE; Schneeberger *et al.*, 2009) and recombination mapping, we narrowed *nde2* down to an interval on chromosome 4 that lacked non-synonymous candidate single nucleotide polymorphisms according to whole-genome resequencing data. However, the candidate interval coincided with the insertion site of the EDS1-YFP^{NLS} transgene (At4g28490; Stuttmann *et al.*, 2016). Thus, suppression of autoimmunity in *nde2* is most likely caused by downregulation of EDS1-YFP^{NLS} expression. Identification of causal mutations in remaining *nde* lines was not attempted.

Targeting of *DM2h* in most *nde* lines suggests that autoimmune induction by EDS1-YFP^{NLS} does not require additional *DM2*-encoded NLRs. We demonstrated this also by comparing autoimmunity in near-isogenic lines ectopically expressing *DM2h* and containing *DM2*^{Ler} or *DM2*^{Col} (Figure 1b,c). A complementation line expressing *DM2h*

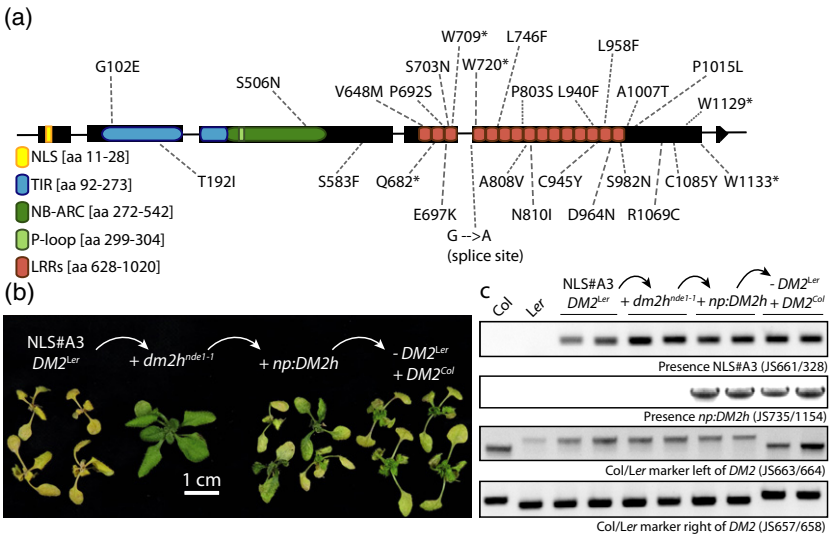

Figure 1. *DM2h* is the main locus targeted by the *nde* suppressor screen, and is sufficient for EDS1-YFP^{NLS}-induced autoimmunity.
(a) Protein motifs, domain boundaries and mutations discovered in different *nde* alleles parsed on to the *DM2h* gene model are shown (drawn to scale; gDM2h: 4031 nt ATG->STOP). In total, 15 leucine-rich repeats (LRRs) are predicted for DM2h by LRRpredictor (Martin *et al.*, 2020a).
(b) *DM2a-g*^{Ler} is not required for autoimmunity induced by EDS1-YFP^{NLS}. Plants were grown under high temperature conditions, and shifted to 18/16°C to induce autoimmunity for 8 days before documentation. The NLS#A3 line (parental line used for the *nde* suppressor screen) expresses EDS1-YFP^{NLS} under *EDS1* promoter control in the Col *eds1-2* genetic background (a near isogenic line containing the *DM2*^{Ler} region). The *dm2h*$^{nde1-1}$ allele was isolated from the suppressor screen, and was subsequently complemented by a T-DNA for expression of g*DM2h* under control of its own promoter (+ *np:DM2h*). From a cross to Col, a line containing both transgenes (EDS1-YFP^{NLS}, *DM2h*), but not the *DM2*^{Ler} region, was isolated.
(c) Polymerase chain reaction genotyping of lines used in (b), showing presence/absence of the two transgenes (EDS1-YFP^{NLS}, *np:DM2h*) and origin (Col, L*er*) of the *DM2* region.

under control of its native promoter in the *dm2h*$^{nde1-1}$ background (Col *eds1-2 dm2h*$^{nde1-1}$ *np:gEDS1-YFP*^{NLS} *np:gDM2h*; Col *eds1-2* is a near isogenic line that also contains *DM2*^{Ler}) (Stuttmann *et al.*, 2016) was crossed to Col, and lines containing *DM2*^{Col} and both transgenes were selected (*EDS1-YFP*^{NLS}, *DM2h*; Figure 1c). Autoimmunity was induced similarly when plants containing *DM2*^{Ler} or *DM2*^{Col} (and ectopically expressing DM2h and EDS1-YFP^{NLS}) were shifted to low temperatures (Figure 1b). Thus, the *DM2a-g* genes from the *DM2*^{Ler} region have weak or no contribution to necrosis induction, and *DM2h* is necessary and sufficient for autoimmunity induced by EDS1-YFP^{NLS}.

Generation of *DM2*^{Ler} mutant variants by genome editing

To dissect the functions of *DM2* genes in autoimmunity and resistance to pathogens, we generated derivatives of the *DM2*^{Ler} cluster by genome editing (Ordon *et al.*, 2017, 2019). The genetic makeup of mutant lines is summarized in Figure 2 (see Figure S2 for details). *dm2c-4* and *dm2h-1* are single mutant lines. The *Δdm2a-g* mutant line expresses only *DM2h* from its native genomic locus. *Δdm2-11* (approximately 70 kb deletion) and *Δdm2-3* (approximately 120 kb deletion) lack all *DM2* genes, but also regions encompassing At3g44610-620 and At3g44680-700 were deleted in *Δdm2-3* (Figure 2). Some mutant lines were initially generated in the *old3-1* mutant background, and wild-type *OLD3* (OASTL-A1; AT4G14880) was subsequently introduced by crossing to L*er* (Ordon *et al.*, 2017; Tahir *et al.*, 2013). Notably, *Δdm2-3* mutant plants (lacking *DM2* and flanking genes) were smaller at the seedling stage up to approximately 3–4 weeks and flowered earlier than control plants under short day conditions (Figure S2). These phenotypes were independent of *OLD3/old3-1*, and were not detected in *dm2-11* plants. Thus, the observed differences are likely due to deletion of the cluster-flanking genes in *Δdm2-3*.

The *DM2*^{Ler} region contributes to oomycete resistance, but this is independent of the RPP1-like NLRs

Maintenance of the *DM2*^{Ler} haplotype in the natural populations despite its potentially detrimental effects on plant fitness in combination with certain genetic backgrounds (Alcazar *et al.*, 2014; Atanasov *et al.*, 2018) suggests it may confer selective advantages. We tested a potential role of the *DM2*^{Ler} region in natural pathogen resistance by challenging Δ*dm2-3* mutant plants (lacking *DM2* and flanking genes) with virulent *Pseudomonas syringae* bacteria (*Pst* DC3000; Figure 3a) and compatible and incompatible *Hpa* isolates Cala2 and Emwa1, respectively (Figure 3b,c). The L*er rar1-13* line was included as a control for moderately impaired immunity (Muskett *et al.*, 2002). As expected, *Pst* DC3000 bacteria grew better in *rar1-13* mutant plants, and in *old3-1* mutant plants (compare *Δdm2-3* and *Δdm2-3*

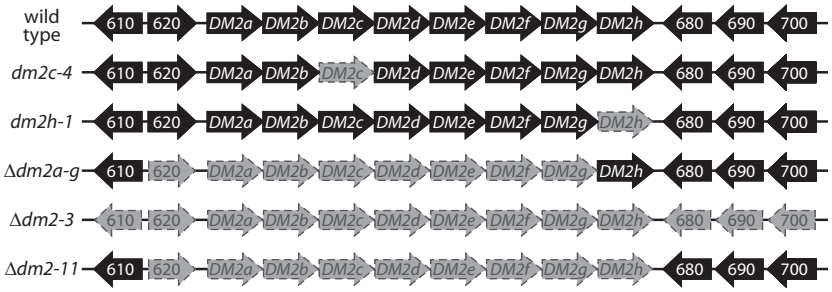

Figure 2. *dm2* mutant Arabidopsis lines used in this study.
Schematic drawing of the *DM2*^{Ler} region. Gene identifiers are the last three digits of At3g44xxx. Genes present in respective lines are depicted in black, and genes deleted or inactivated in mutant lines are shown in gray. Details on mutant lines are provided in Figure S2.

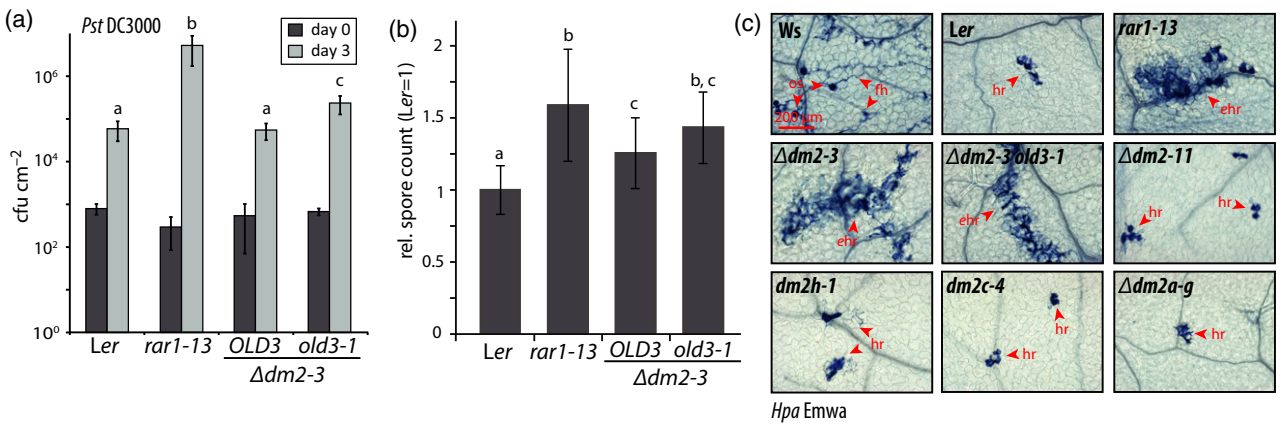

Figure 3. Infection of *dm2* mutant lines with bacterial and oomycete pathogens.
(a) Indicated plant lines were challenged with virulent *Pst* DC3000 bacteria, and bacterial titers determined at 0 and 3 dpi. Error bars indicate standard deviation of eight replicates, letters indicate statistically significant differences at day 3 as determined by one-way ANOVA and Fisher LSD ($P < 0.001$). The experiment was conducted three times with similar results; one representative experiment is shown.
(b) Indicated plant lines were challenged with virulent *Hyaloperonospora arabidopsidis* (*Hpa*) isolate Cala2. Sporulation was assessed at 7 dpi to quantify pathogen growth. The experiment was conducted four times with four replicates. Data were normalized by arbitrarily setting sporulation on L*er* = 1, and all 16 replicates were included in the analysis. Error bars and statistics as in (a).
(c) Infection phenotypes of indicated plant lines after challenge with *Hpa* isolate Emwa1, avirulent on L*er*. First true leaves were stained with Trypan blue at 6 dpi. The experiment was conducted five times. Representative micrographs are shown. ehr, expanded hr; fh, free hyphae; hr, hypersensitive response; os, oospores. Scale bar = 200 µm.

old3-1; Tahir *et al.*, 2013). However, *Pst* DC3000 grew to similar levels in wild-type and *Δdm2-3* mutant plants, indicating that the *DM2*^{Ler} haplotype does not contribute to *Pst* DC3000 resistance (Figure 3a). In contrast, Δ*dm2-3* mutant plants supported higher sporulation of the compatible *Hpa* isolate Cala2, and this phenotype was aggravated by presence of *old3-1* (Figure 3b). Similarly, isolate Emwa1, which is resisted by *RPP4/RPP8* in accession L*er* (Holub *et al.*, 1994), showed enhanced outgrowth at infection sites and provoked less-confined, expanded HRs in *Δdm2-3* mutant plants in comparison with wild-type L*er* (Figure 3c). This phenotype was more severe than that of the *rar1-13* mutant, which was only weakly impaired in resistance to Emwa1 under our conditions.

We assumed that one or several *Hpa* effectors might be weakly recognized by RPP1-like NLRs encoded at the *DM2*^{Ler} locus. We used infection with the *Hpa* isolate Emwa1 and Trypan blue staining to analyze contributions of *DM2*^{Ler} genes to *Hpa* resistance in more detail (Figure 3c). *Δdm2a-g*, *dm2c* and *dm2h* mutant plants were not impaired in resistance (Figure 3c). Unexpectedly, also the *Δdm2-11* mutant line, which carries a deletion of all *DM2* genes, was as resistant as L*er* wild type to *Hpa* Emwa1 (Figure 3c). This suggests that one of the flanking genes present in *Δdm2-11*, but absent in *Δdm2-3* (Figure 2), directly or indirectly contributes to *Hpa* resistance. *HISTONE DEACETYLASE9* (At3g44680) may be a most likely candidate, as it was reported to regulate flowering time (Figure S2; Kim *et al.*, 2013; Park *et al.*, 2019) and plant resistance responses (Yang *et al.*, 2020).

DM2h is necessary and sufficient for autoimmunity induced by *old3-1* and *SRF3*$^{Kas/Kond}$

The contribution of individual *DM2*^{Ler} genes to temperature-dependent autoimmunity induced by *old3-1* or *SRF3*$^{Kas/Kond}$ was not fully clarified (Alcazar *et al.*, 2009, 2010; Atanasov *et al.*, 2018; Stuttmann *et al.*, 2016; Tahir *et al.*, 2013). We therefore analyzed lines containing *old3-1* or *SRF3*^{Kond} and varying complements of *DM2* genes for autoimmune induction at low temperature (Figure 4).

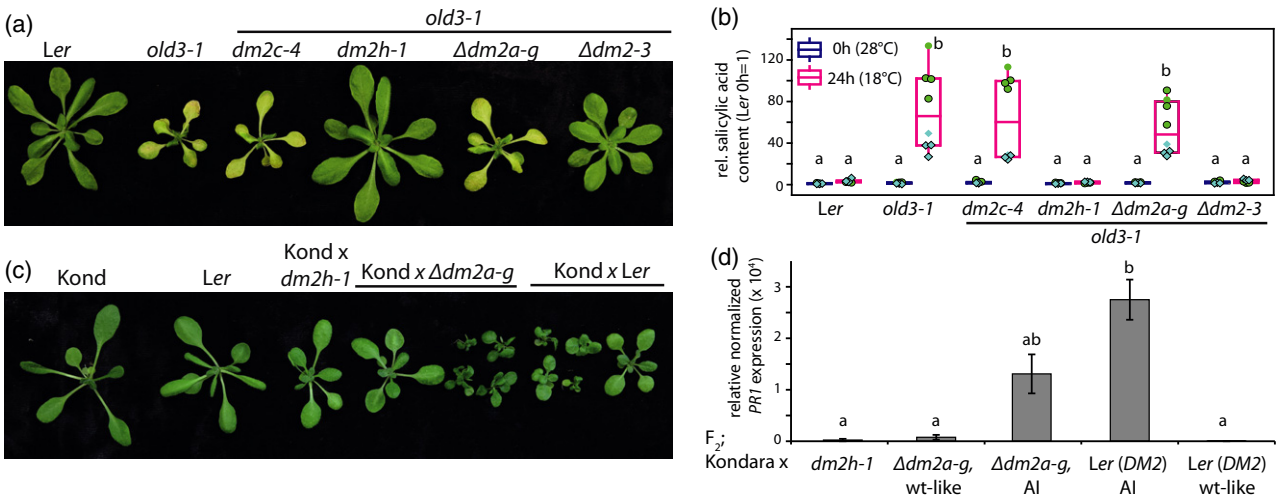

Figure 4. *DM2h* from the *DM2*^{Ler} cluster is sufficient for autoimmune induction by *old3-1* or *SRF3*^{Kond}.
(a) Contribution of *DM2* genes to *old3-1*-induced autoimmunity. Plants were grown for 7 days under short day conditions, shifted for 14 days to 28°C, and then shifted to 18/16°C. Phenotypes were documented 7 days after temperature shift.
(b) Relative (L*er* 0 h = 1) salicylic acid accumulation in leaf tissue of indicated plants lines at 28°C and 24 h after shift to 18/16°C. The experiment was conducted twice (green and cyan data points, respectively) with four replicates per experiment. Letters indicate statistically significant differences (ANOVA, Tukey *post-hoc* test, $P < 0.001$).
(c) Contribution of *DM2* genes to *SRF3*^{Kond}-induced autoimmunity. Control plants (Kond, L*er*) and F_2 populations of the indicated crosses were grown under low temperature regime (14°C/12°C day/night; short day). Representative plants were documented after 7 weeks, and both wild type-like and autoimmune plants are shown for segregating populations. Crosses were verified by polymerase chain reaction genotyping (Figure S3).
(d) Expression of the marker gene *PR1* in F_2 plants from indicated crosses (to Kondara) as measured by quantitative reverse transcription–polymerase chain reaction. For crosses of Kond to L*er* and *Δdm2a-g*, wild-type (wt)-like and autoimmune (AI) plants were analyzed. Means and standard errors of three biological replicates are shown. The experiment was conducted twice with similar results. Statistics as in (b).

Different lines were compared phenotypically 7 days after a temperature shift, and SA levels or defense marker transcript levels were determined 24 h after a temperature shift to assess autoimmunity induction quantitatively. There were no phenotypic differences between *old3-1* plants expressing only *DM2h* from its native genomic locus (*Δdm2a-g old3-1*) or those also containing additional *DM2* genes (Figure 4a,b). However, SA levels were mildly reduced in *Δdm2a-g old3-1* plants after temperature shift compared with *old3-1* plants (Figure 4b). Similarly, autoimmune hybrids obtained from crosses to Kondara (to introduce *SRF3*^{Kond}) and containing either the full *DM2*^{Ler} cluster or only *DM2h* (in the *Δdm2a-g* line) were phenotypically indistinguishable, and expression of the defense marker gene *Pathogenesis Related 1* (*PR1*) was slightly reduced in necrotic hybrids lacking *DM2a-g* (Figure 4c,d; Figure S3). In conclusion, the data do not suggest a major role for *DM2a-g*. Thus, *DM2h* is sufficient for autoimmune induction not only by EDS1-YFP^{NLS} (Figure 1), but also by *old3-1* and *SRF3*^{Kond}.

Functional analysis of DM2h

Our genetic analyses showed that DM2h mediates autoimmunity induced by EDS1-YFP^{NLS}, *old3-1* and *SRF3*$^{Kas/Kond}$ (Figures 1 and 4). We wondered whether there were mechanistic differences between the risky DM2h NLR, prone to autoimmune induction, and previously characterized sensor TNLs. Therefore, we conducted functional analyses of DM2h.

We relied on heterologous expression in *Nb* (by agroinfiltration) for functional analysis. On the one hand, we used a TIR domain fragment, DM2h$_{1\text{-}279}$, which induces *EDS1*-dependent cell death in *Nb* (Gantner *et al.*, 2019). On the other hand, we developed a co-expression assay to interrogate functionally the DM2h full-length protein (Figure S4): expression of DM2h together with EDS1-YFP^{NLS} or old3-1, but not expression of the proteins alone or co-expression of DM2h with EDS1-YFP or OLD3, induced HR-like cell death in *Nb*. Co-expression of DM2h with SRF3^{Kond}, described to provoke autoimmunity recessively and only in absence of a compatible *SRF3* allele in Arabidopsis (Alcazar *et al.*, 2010), did also not induce HR-like cell death. Thus, cell death induction in *Nb* faithfully recapitulated activation of DM2h-dependent autoimmunity in Arabidopsis, and can be used as a proxy for DM2h activation and initiation of TNL-mediated defenses.

DM2h encompasses an additional 5′ exon present in some *RPP1* homologs (Figure 1a; Chae *et al.*, 2014; Meyers *et al.*, 2003). The encoded N-terminal extension contains a predicted myristoylation motif (including the critical G2 residue) and a bipartite nuclear localization signal (Stuttmann *et al.*, 2016). Furthermore, DM2h contains a GK di-

residue critical for ATP binding within the P-loop and a characteristic SH motif predicted to be required for TIR-TIR interactions (Bonardi *et al.*, 2011; Burdett *et al.*, 2019; Williams *et al.*, 2014).

A variant of a DM2h$_{1-279}$-green fluorescent protein (GFP) fusion carrying exchanges (to alanine) in the SH motif (SH-AA) accumulated to wild-type levels on Western blots, but did not induce cell death anymore (Figure 5a,b),

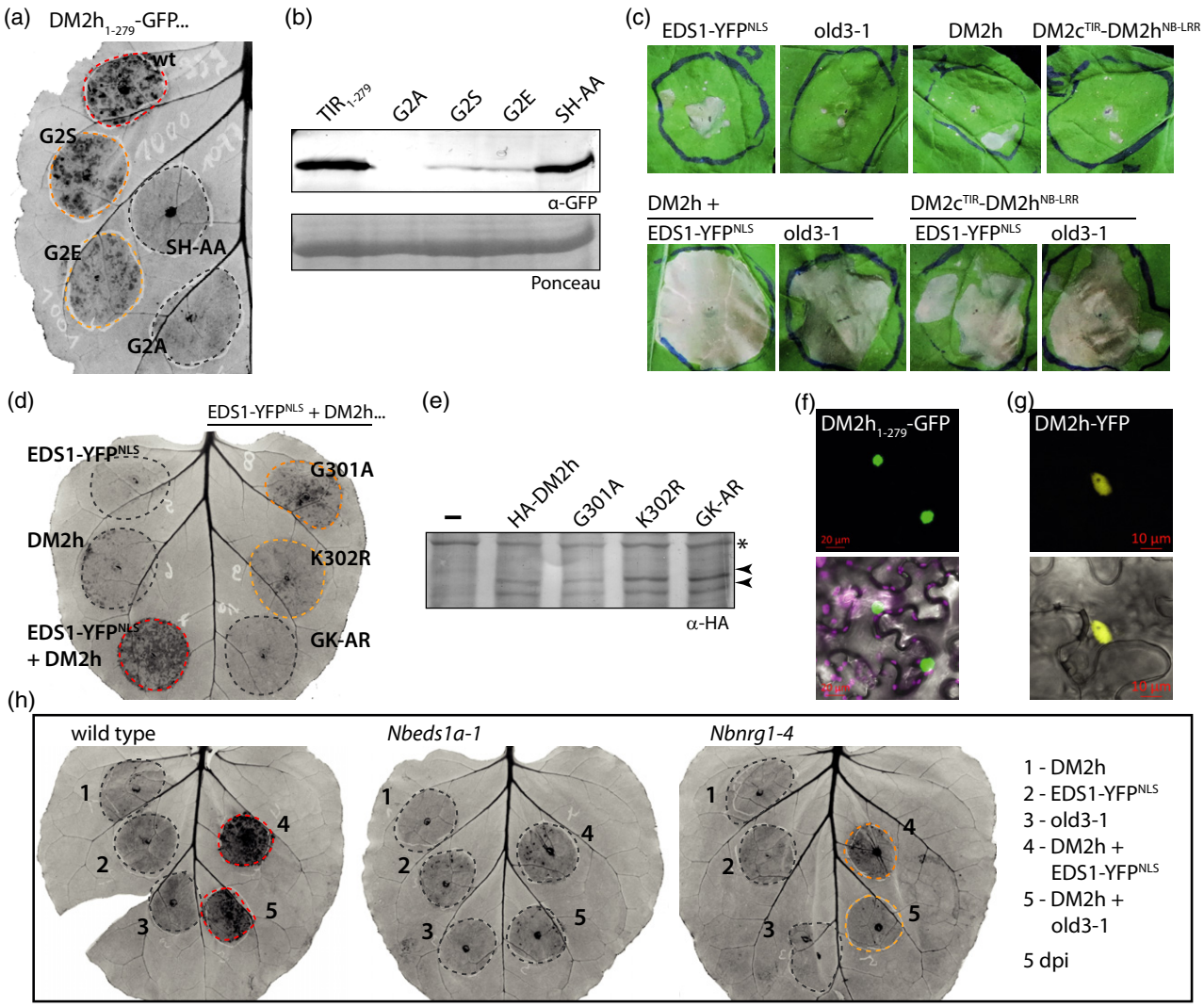

Figure 5. Functional analysis of the DM2h receptor.
(a) Cell death induction by DM2h$_{1-279}$ and variants thereof in leaves of wild-type *Nicotiana benthamiana*. TIR domain fragments were expressed with a C-terminal green fluorescent protein (GFP) tag (35S:DM2h$_{1-279}$-GFP), and plant reactions were documented at 4 dpi.
(b) Immunodetection and accumulation of proteins transiently expressed in (a).
(c) Cell death induction upon (co-)expression of DM2h or a DM2c/DM2h chimeric protein together with EDS1-YFP^{NLS} or old3-1. After agroinfiltration, plants were incubated in the dark for 2 days, plant reactions were documented at 5 dpi. YFP. yellow fluorescent protein.
(d) P-loop dependency of DM2h-mediated cell death. DM2h and P-loop variants, as indicated and without an epitope tag, were expressed by agroinfiltration, and cell death induction was imaged at 5 dpi.
(e) Immunodetection and accumulation of DM2h P-loop variants. Constructs similar to those used in (d) but encoding an N-terminal 6× hemagglutinin (HA) tag were used for agroinfiltration. Protein extracts were prepared at 3 dpi. Arrowheads mark two DM2h-specific signals. A non-specific signal, marked by an asterisk, is shown as loading control.
(f) Subcellular localization of the DM2h$_{1-279}$ TIR domain fragment in *N. benthamiana*. GFP channel (upper panel) and a merged image (lower panel) including bright field and chlorophyll imaging (magenta) are shown. Similar results were obtained upon expression in *Nbeds1*. Scale bar = 20 µm.
(g) Subcellular localization of a DM2h-YFP fusion protein in transgenic Arabidopsis (Col *p35S:gDM2h-YFP*). Fourteen-day-old plants grown in short day conditions were used for imaging. With identical microscope settings, no fluorescence signal was detected in control plants. Multiple plants were analyzed; a representative micrograph is shown. Immunodetection of the DM2h-YFP fusion protein and growth phenotype of the transgenic line in Figure S5.
(h) DM2h-mediated cell death induction is dependent on the TNL downstream signaling components *EDS1* and *NRG1*. As in (d), but different *N. benthamiana* mutant lines were used in co-expression assays. Details on the *nrg1-4* mutant line in Figure S6.

suggesting that cell death activity may involve TIR-TIR interactions. A DM2h$_{1\text{-}279}$-GFP G2A variant was not stable (Figure 5b). G2S and G2E variants accumulated to low levels, but still induced residual cell death (Figure 5a,c), arguing against a requirement for myristoylation. This was further examined by co-expressing a DM2c^{TIR}-DM2h$^{NB\text{-}LRR}$ chimeric protein together with EDS1-YFP^{NLS} and old3-1 (Figure 5c). DM2c is highly similar to DM2h (approximately 80% amino acid identity in the region encoded by the DM2c/h chimeric construct), but lacks the N-terminal extension of DM2h and does not contain a predicted myristoylation motif or NLS. In co-expression assays, the DM2c^{TIR}-DM2h$^{NB\text{-}LRR}$ chimeric protein could mediate EDS1-YFP^{NLS}- and old3-1-induced cell death, although this was mildly reduced in comparison with co-expression of native DM2h (Figure 5c). Taken together, these data suggest that the G2 residue is critical for stability, while myristoylation is not required for cell death executed by DM2h. Furthermore, DM2h P-loop variants (G301A, K302R) were tested in co-expression assays (Figure 5d). While single amino acid exchanges strongly reduced the DM2h cell death activity, it was fully abolished when both residues were simultaneously exchanged in DM2h (GK-AR). DM2h, which often produced two signals on Western blots, and P-loop variants accumulated to similar levels, suggesting that amino acid exchanges did not impair protein stability (Figure 5e; please note that cell death assays were conducted with untagged proteins, as tagged variants (e.g., N- and C-terminal 6× hemagglutinin and GFP tags tested) were not or only weakly functional in this system).

In addition, we aimed to determine the subcellular localization of DM2h by live cell imaging. No fluorescence signal was detected when the full-length protein, in fusion to GFP, was expressed by agroinfiltration. However, strong fluorescence in nuclei was observed when the DM2h$_{1\text{-}279}$-GFP TIR fragment was expressed in *Nb* (Figure 5f). Similarly, DM2h was detected primarily in nuclei when examining a transgenic Arabidopsis line expressing DM2h-YFP under 35S promoter control in accession Col (Figure 5g; Figure S5).

Last, we determined the genetic requirements of DM2h-mediated cell death in *Nb* co-expression assays using an *Nbeds1* line and a newly generated *Nbnrg1* mutant line (Figure S6). Plant reactions induced upon co-expression of DM2h with EDS1-YFP^{NLS} or old3-1 were fully and partially abolished in *eds1* and *nrg1* mutant plants, respectively (Figure 5h).

In conclusion, our data suggest that induction of immune responses by DM2h may involve TIR-TIR interactions and requires an intact P-loop (Figure 5c,d), but not myristoylation (Figure 5a,c). Potential myristoylation is also not supported by localization studies, which suggest the nucleus as the predominant compartment for DM2h (Figure 5f,g). Induction of downstream resistance responses by DM2h, here tested in *Nb*, requires EDS1 complexes and the helper NLR NRG1 (Figure 5h). Thus, our data do not support mechanistic differences between the autoimmune risk NLR DM2h and classical sensor NLRs, as they recapitulate previously reported analyses of RPP1 orthologs functioning in *Hpa* resistance (Krasileva *et al.*, 2010; Schreiber *et al.*, 2016; Zhang *et al.*, 2017) and other sensor TNLs (e.g., Burch-Smith *et al.*, 2007; Saile *et al.*, 2020; Williams *et al.*, 2014; Wirthmueller *et al.*, 2007).

EDS1-YFP^{NLS} operates upstream of DM2h

EDS1, in its function as an immune regulator, is assumed to signal at the level of or immediately downstream of activated TNL-type receptors. However, *Nb* co-expression assays (Figure 5) place *At*EDS1-YFP^{NLS} upstream of DM2h in cell death induction, as Arabidopsis EDS1 cannot exert immune signaling in *Nb* (Gantner *et al.*, 2019; Lapin *et al.*, 2019). This is also supported by the fact that EDS1-YFP^{NLS}-induced cell death is abolished in *Nbeds1* plants (Figure 5h).

We made use of a previously identified loss-of-function allele of Arabidopsis EDS1, EDS1(F419E), to disentangle EDS1 functions in downstream immune signaling from its role in the activation of DM2h in the context of the EDS1-YFP^{NLS} fusion protein. EDS1(F419E) corresponds to a mutation identified in tomato EDS1, *Sl*EDS1(F435E), which abolishes EDS1 signaling functions, but does not interfere with assembly of EDS1 complexes with PAD4 or SAG101 (Gantner *et al.*, 2019; Lapin *et al.*, 2019). When expressed together with DM2h in *Nb*, EDS1-YFP^{NLS} and the corresponding F419E variant induced cell death to similar extents, while EDS1-YFP and EDS1-YFP^{nls} did not (Figure 6a). We also analyzed positioning of EDS1-YFP^{NLS} in Arabidopsis autoimmune induction by temperature shift experiments using primary transformants (Figure 6b). EDS1-YFP^{NLS} and an EDS1-YFP^{NLS}(F419E, L258A, L262A) variant (under native promoter control) were combined with DM2h by transforming the constructs into wild-type L*er* plants and/or the L*er eds1-2* mutant line. The L258A and L262A exchanges reduce the affinity of EDS1 to PAD4 and SAG101 (Wagner *et al.*, 2013). They were combined with F419E in the transformation construct to avoid dominant negative effects from interference with the assembly of endogenous EDS1-PAD4/SAG101 complexes. EDS1-YFP^{NLS} induced autoimmunity among primary transformants in the L*er eds1-2* background, as expected (Figure 6b). In contrast, EDS1-YFP^{NLS}(F419E, L258A, L262A) did not induce autoimmunity in *eds1-2* plants, but in wild-type L*er* background (Figure 6b). This confirms that EDS1 (F419E) is not functional in downstream immune signaling (Lapin *et al.*, 2019), and shows it is still capable of activating DM2h to induce autoimmunity in the presence of signaling-competent, endogenous EDS1 complexes in Arabidopsis. The F419E mutation did not interfere with

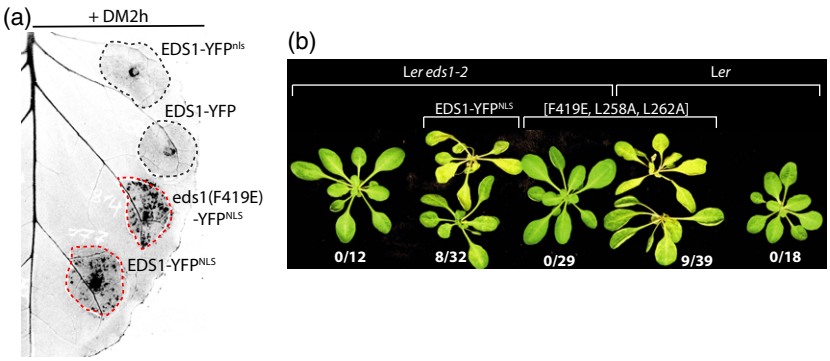

Figure 6. Activation of DM2h by EDS1-YFP^{NLS} is independent of EDS1's role in signal transduction.
(a) Induction of HR-like cell death by different EDS1-YFP fusion protein variants in *Nicotiana benthamiana*. Indicated EDS1 variants were expressed together with DM2h, and cell death was imaged at 6 dpi. Immunodetection of proteins and subcellular localization in Figure S7. YFP. yellow fluorescent protein.
(b) Induction of autoimmunity by EDS1-YFP^{NLS} fusion protein variants. Transgenes for the expression of immune-competent EDS1-YFP^{NLS} or the non-functional EDS1-YFP^{NLS}(F419A, L258A, L262A) variant under control of the native promoter were transformed into accession L*er* or the L*er eds1-2* mutant line. Transgenic seeds were selected by FAST seed fluorescence. Plants were first grown 4 weeks under immune-suppressive conditions, and autoimmune induction was evaluated and documented 6 days after shift to 18/16°C. Numbers indicate frequencies of autoimmune plants. Expression of transgenic proteins and presence/absence of endogenous EDS1 was shown on immunoblots (see Figure S7c).

protein stability or alter protein subcellular localization (Figure S7). Thus, cell death-based *Nb* assays and stable Arabidopsis transformants provide strong evidence for a position of EDS1-YFP^{NLS} upstream of DM2h in the activation of the immune receptor. Concomitantly, we conclude that DM2h activation by EDS1-YFP^{NLS} is unrelated to and independent of EDS1 immune signaling functions, albeit DM2h, as a classical TNL, requires EDS1 signaling functions for downstream signal relay.

Identification of features within EDS1-YFP^{NLS} required for DM2h activation

The observations that DM2h functions similar to NLRs conferring natural pathogen resistance (Figure 5) and that EDS1-YFP^{NLS} operates upstream of the DM2h immune receptor (Figure 6) suggest that the fusion protein might mimic an effector activating a sensor NLR. We therefore hypothesized that EDS1-YFP^{NLS} contained a surface or epitope-like feature specifically recognized by the DM2h immune receptor.

We generated EDS1 expression constructs differing in the NLS (as EDS1-YFP did previously not induce autoimmunity; Figure 5; Stuttmann *et al.*, 2016) or the linker connecting EDS1 with the YFP moiety (Figure 7a). Expression constructs encoded for an SV40 NLS lacking two terminal glycine residues, which were contained in the original EDS1-YFP^{NLS} fusion, or an NLS from c-myc, the human cancer protein. In addition, constructs encoded either a 16 amino acid linker derived from the Gateway attB recombination site, or a short Ala-Ser-Ala (ASA) linker (Figure 7a). When tested in *Nb* co-expression assays, all fusion proteins containing the Gateway-linker activated DM2h and induced cell death, while those containing the ASA linker did not (Figure 7b). EDS1-YFP^{NLS} variants showed similar subcellular localizations, and were not impaired in protein accumulation (Figure S8). EDS1-YFP^{NLS} variants were further tested for their capacity to mediate TNL signaling and to induce autoimmunity in Arabidopsis. Constructs for expression of EDS1-YFP^{NLS} variants, under *EDS1* promoter control, were transformed into the Col *eds1-2* line (containing DM2^{Ler}; Figure 1b,c). Infection studies with primary transformants and *Hpa* isolate Cala2 showed that all variants could complement impaired *RPP2*-mediated resistance of the Col *eds1-2* line, and were thus functional in the context of downstream TNL signaling (Figure 7c). However, in agreement with results obtained in *Nb* co-expression assays, only those variants containing the Gateway linker also induced autoimmunity in temperature-shift experiments (Figure 7d). Thus, minor differences within the EDS1-YFP^{NLS} fusion protein differentiate a DM2h-activating variant from one that is compatible with DM2h. These differences are not linked to EDS1 immune signaling functions.

DISCUSSION

A number of NLR-coding loci, often referred to as risk loci or *DANGEROUS MIX* loci, are involved in the induction of autoimmunity in diverse scenarios. Among these, DM2^{Ler} is unique because of its role in at least three independent cases of autoimmunity, in genetic interactions with natural and EMS-induced alleles, or an ectopically expressed EDS1-YFP^{NLS} protein (Alcazar *et al.*, 2009; Stuttmann *et al.*, 2016; Tahir *et al.*, 2013). In this study, the *DM2h* gene from the *DM2*^{Ler} cluster was not only identified as the exclusive target of our EDS1-YFP^{NLS} suppressor screen (Figure 1), but also revealed as the major driver of autoimmune induction when expressed from its endogenous genomic locus (in a *Δdm2a-g* mutant line) together with *old3-1* or

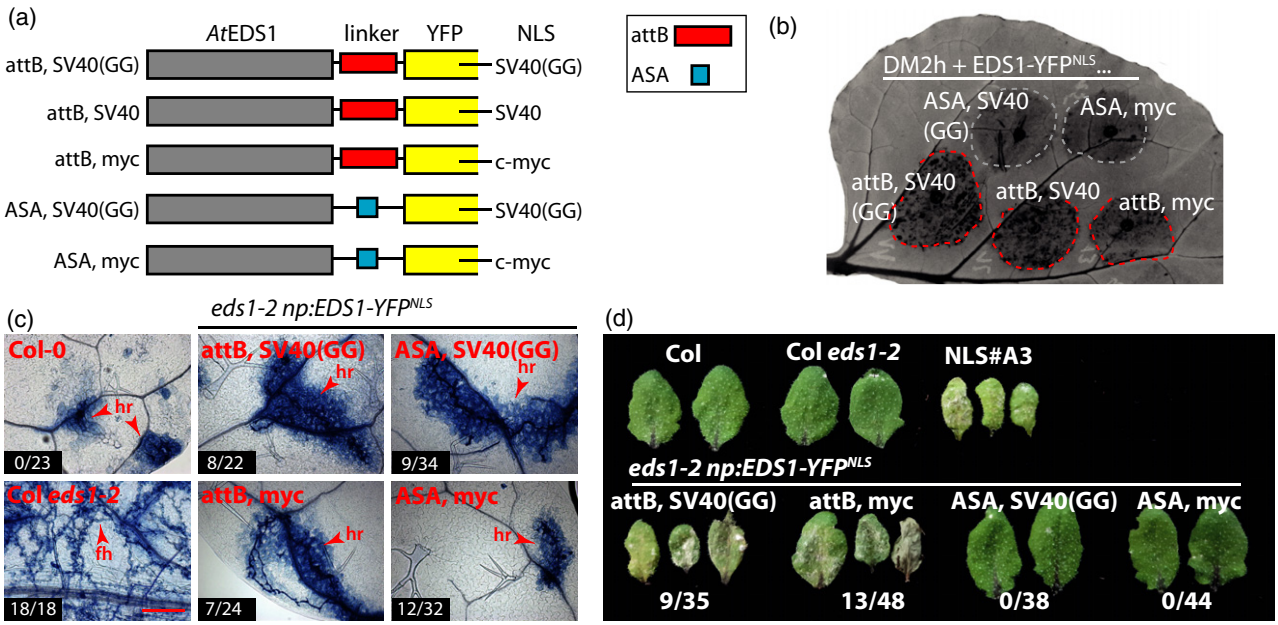

Figure 7. Analysis of EDS1-YFP^{NLS} properties required for activation of DM2h.
(a) Schematic representation of different EDS1-YFP^{NLS} variants compared for their capacity to activate DM2h. Red box represents the Gateway linker (KGGRADPAFLYKVVDG), blue box an Ala-Ser-Ala (ASA) linker. Precise sequence of used NLSs is as follows: SV40 – PKKKRKV*; SV40(GG) – PKKKRKVGG*; c-myc – SAPAAKRVKLD*. Short names indicated with constructs are used throughout the figure panels. YFP. yellow fluorescent protein.
(b) Induction of DM2h-mediated HR-like cell death by different EDS1-YFP^{NLS} variants in *Nicotiana benthamiana* co-expression assays. Plant reactions were imaged at 5 dpi. Subcellular localization and accumulation of fusion proteins are shown in Figure S8.
(c) Functionality of EDS1-YFP^{NLS} variants in TNL signaling. Indicated variants were transformed, under control of the native *EDS1* promoter, into the Col *eds1-2* line. Primary transformants were selected by FAST seed fluorescence. Plants were grown for 7 days under short day conditions and 10 days under high temperature conditions before infection with *Hyaloperonospora arabidopsidis* Cala2. First true leaves were Trypan blue-stained at 6 dpi, and representative micrographs are shown. Numbers indicate plants with macroscopically visible sporulation. fh, free hyphae. Scale bar = 200 μm.
(d) Autoimmune induction by EDS1-YFP^{NLS} variants. As in (c), but plants were grown 7 days under short day conditions, 20 days under high temperature conditions and were then shifted to low temperature (18/16°C) for 5 days, before documentation of autoimmune induction. Numbers indicate frequency of autoimmune plants among the total number of primary transformants that were analyzed. The experiment was performed twice. Frequencies for autoimmune plants were similar and total numbers from both replicates are indicated.

SRF3^{Kond} (Figure 4; Atanasov *et al.*, 2018). Thus, we demonstrate that a single NLR is necessary and sufficient in all three scenarios of autoimmune induction. This raises the questions how autoimmune risk NLRs may be different from classical sensor NLRs and how DM2h becomes activated in the presence of different incompatible alleles.

Sensor NLRs versus risk-NLRs: any evidence for conceptual differences?

RPP1-like NLRs encoded at the *DM2* locus in Arabidopsis accessions and conferring resistance to different *Hpa* isolates were extensively characterized in previous studies (Chou *et al.*, 2011; Goritschnig *et al.*, 2016; Horsefield *et al.*, 2019; Krasileva *et al.*, 2010; Rehmany *et al.*, 2005; Schreiber *et al.*, 2016; Steinbrenner *et al.*, 2015; Wan *et al.*, 2019; Zhang *et al.*, 2017). In addition, the structure of activated RPP1^{WsB} in complex with its recognized effector was recently reported (Ma *et al.*, 2020). Summarizing our current understanding, activation of RPP1-dependent immune responses depends on: (i) direct interaction of the recognized effector with the receptor's LRR and post-LRR domains; (ii) receptor oligomerization, controlled by ATP-binding at the P-loop; (iii) TIR-TIR interactions via the AE and DE interfaces; and (iv) enzymatic (NADase) activity dependent on a critical TIR domain glutamate residue. As for Roq1, formation of the tetrameric resistosome complex regulates RPP1 TIR domain enzymatic activity (Ma *et al.*, 2020; Martin *et al.*, 2020b). Furthermore, RPP1-mediated resistances depend on EDS1 complexes and helper NLRs (Jubic *et al.*, 2019; Qi *et al.*, 2018; Wagner *et al.*, 2013). Here, we reinforce and add to previous analyses of the RPP1-like risk NLRs DM2d^{Uk-1} and DM2h^{Bla-1} (Chae *et al.*, 2014; Tran *et al.*, 2017) by functional analysis of DM2h^{Ler} (Figure 5). Our results support that also DM2h activation depends on a functional P-loop and TIR-TIR interactions. In addition, our *Nb* assays reveal that DM2h-mediated responses are, fully and partially, dependent on presence of EDS1 complexes and the NRG1 helper NLR, respectively. Lastly, we identify the nucleus as the most likely compartment for DM2h localization (Figure 5h,g), which is in agreement with previous analyses of the TNLs N and RPS4 (Burch-Smith *et al.*, 2007; Wirthmueller *et al.*, 2007).

Overall, therefore, our results do not support mechanistic differences between autoimmune risk-NLRs and sensor NLRs characterized in pathogen resistance.

In the absence of mechanistic differences, what could be the basis for the frequent involvement of certain NLR loci, such as *DM2*, in autoimmunity? The *DM2* locus and additional complex *NLR* loci stand out at the genome-scale for their complexity and evolutionary dynamics (Chae *et al.*, 2014; Jiao and Schneeberger, 2020; Lee and Chae, 2020; Van de Weyer *et al.*, 2019). Thus, a disproportionally large number of diversified RPP1-like NLRs may be encoded within the global Arabidopsis gene pool, which may explain to some extent the incidence of *DM2* and other complex *NLR* clusters in autoimmunity. An alternative explanation for why certain highly variable NLRs are particularly prone to autoimmune induction could be that they differ in their activation kinetics. In the equilibrium-based switch model, the NLRs cycle between the ADP-bound OFF and the ATP-bound ON state in the absence of a recognized effector (Bernoux *et al.*, 2016). However, baseline activation levels differ between NLRs, and signaling capacities can be tuned to less responsive or hyper-responsive by altering intramolecular interactions (Bernoux *et al.*, 2016; Qi *et al.*, 2012). Risk NLRs may, at least in some cases, be shifted particularly far towards the ON/hyper-responsive state in comparison with evolved sensor NLRs. This may place them directly at the brink of full activation, so that spurious interactions or even cellular perturbations may be sufficient for immune receptor activation and resistosome formation. The concept of cellular perturbation as an NLR trigger is, e.g., supported by an accession-specific *TNL* allele inducing autoimmunity under osmotic stress (Ariga *et al.*, 2017). Activation of NLRs by altered cell physiology could provide one possible explanation for the apparent promiscuous activation properties of DM2h as well as other risk NLRs, such as SUPPRESSOR OF NPR1-1, CONSTITUTIVE1 (SNC1) (see e.g., Chakraborty *et al.*, 2018).

DM2h as a guardian NLR, or direct binder?

The most plausible scenarios for the induction of DM2h-mediated autoimmunity are direct activation of the DM2h immune receptor through physical interaction with gene products of incompatible alleles or disturbance of guard–guardee pairs (Kourelis and van der Hoorn, 2018; Rodriguez *et al.*, 2016). While experimental data supporting either scenario are scarce, we think that a number of arguments favor direct activation. RPP1 receptors conferring *Hpa* resistance directly bind corresponding ARABIDOPSIS THALIANA RECOGNIZED1 (ATR1) effector proteins via their LRR domain, and variation at *RPP1* and *ATR1* loci and structure–function analyses support ongoing co-evolution of receptor and ligand surfaces (Chou *et al.*, 2011; Goritschnig *et al.*, 2016; Krasileva *et al.*, 2010; Rehmany *et al.*, 2005; Steinbrenner *et al.*, 2015). There does not appear to be any difference *per se* between NLRs encoded at risk loci and those with characterized immune functions, and inducers of autoimmunity demonstrate the same behavior of allele-specific receptor activation as pathogenic ATR1 effectors (Figures 5 and 7; Alcazar *et al.*, 2014; Chae *et al.*, 2014; Tahir *et al.*, 2013). Genetic screens have so far also not revealed further components required for DM2h-mediated autoimmunity, as might be expected for a scenario of indirect activation (this work; Atanasov *et al.*, 2018; Stuttmann *et al.*, 2016). Maybe most significantly, there is little support for a function of DM2h as guardian NLR from an evolutionary perspective. Guardian NLRs can be expected to co-evolve with guardees and thus to experience balancing or purifying selection. In contrast, NLRs directly binding cognate effectors are required to evolve novel specificities rapidly to adapt to newly arising effector alleles, and thus underlie diversifying selection, which is clearly the case for RPP1-like NLRs. Indeed, Prigozhin and Krasileva (2021) recently proposed that refined NLR clade assignment, coupled with the analysis of amino acid diversity in near-allelic series, can be used to discriminate guardian NLRs and direct binders computationally (Prigozhin and Krasileva, 2021). In this analysis, a class of highly variable NLRs contained all the described Arabidopsis autoimmune loci (including *DM2h*), but not a single known guard NLR (Prigozhin and Krasileva, 2021).

It is also worth noting that two of the EMS-induced *dm2h* alleles identified in the *nde* mutants, E697K and S703N (Figure 1), locate to the presumably surface-exposed positions on the concave surface of the DM2h-LRR domain (variable positions within the LxxLxLxx LRR consensus sequence, prediction of DM2h LRRs using NLR predictors; Martin *et al.*, 2020a). These mutations may highlight an interface for the binding of EDS1-YFP^{NLS} on the DM2h-LRR, and it will be interesting to test whether the respective alleles might be specific for EDS1-YFP^{NLS} recognition; in other words, whether they maintain responsiveness to old3-1 and/or *SRF3*^{Kond}. Furthermore, a total of six independent *dm2h* alleles (including two minor truncations) also highlight the importance of the C-terminal post-LRR domain for autoimmune induction by EDS1-YFP^{NLS}. In the recently solved Roq1 and RPP1 cryo-EM structures, the post-LRR domains contribute to ligand binding together with the LRR (Ma *et al.*, 2020; Martin *et al.*, 2020b).

We could not find any support for direct interaction of old3-1 and EDS1-YFP^{NLS} with DM2h or domains thereof in initial yeast two-hybrid and co-immunoprecipitation assays (not shown). However, more sensitive interaction assays suitable for transient interactions, such as split Luciferase or proximity labeling by TurboID (Arora *et al.*, 2020; Branon *et al.*, 2018; Luker *et al.*, 2004; Mair *et al.*, 2019), may be required for revealing a direct interaction between DM2h and inducers, as it is known that also NLR-effector interactions in pathogen recognition are often highly

transient and difficult to capture experimentally (Saur *et al.*, 2019; Song *et al.*, 2020).

Role of autoimmunity risk loci in natural pathogen resistance: adaptive benefits?

Despite the potential risk of autoimmunity posed by the highly variable NLRs, they are maintained in the natural gene pool (Alcazar *et al.*, 2014; Bomblies and Weigel, 2007). This suggests they may provide selective advantages in a given environment, potentially also due to a low activation threshold. Here, using CRISPR/Cas lines with different complements of *DM2* genes, we failed to show any role of this locus in pathogen resistance (Figure 3). This is reminiscent of a previous analysis of *DM2* haplotypes (Atanasov *et al.*, 2018). However, in addition to evolutionary and population genetics analyses supporting functional relevance of risk loci (e.g., Chae *et al.*, 2014), amino acid diversity within the LRRs of highly variable NLRs supports that variation does not occur randomly, but is the result of underlying selective pressure. For example, amino acid diversity is higher at surface-exposed positions within the LRR fold and often involves hydrophobic residues that may mediate protein–protein interactions (Prigozhin and Krasileva, 2021). Lastly, considering that risk loci are commonly selected for in breeding programs (Bomblies and Weigel, 2007), we most likely lack appropriate pathosystems to detect beneficial functions of risk loci, or effects may be subtle or masked by redundancy in incompatible interactions. To that end, recent system analyses suggest that 68% of plant pathogenic *Pseudomonas* strains are resisted by multiple NLRs in Arabidopsis (Laflamme *et al.*, 2020).

Activation of risk-NLRs by incompatible alleles: EDS1-YFP^{NLS} as a case study

Our data show that, although EDS1 is a well-known immune regulator required for signaling downstream of activated TNLs, the EDS1-YFP^{NLS} fusion protein operates upstream of the DM2h immune receptor to induce autoimmunity (Figures 5 and 6). DM2h activation depends on very specific properties of the fusion protein, i.e., the presence of the Gateway-linker and an NLS, but is independent of EDS1 immune signaling functions (Figures 6 and 7). Theoretically, DM2h activation could result from disturbance of a guard–guardee pair, EDS1-NLR interactions were reported and guarding of EDS1 proposed (e.g., Bhattacharjee *et al.*, 2011; Huh *et al.*, 2017), but, in particular, heterologous *Nb* assays argue otherwise. Case in point, DM2h activation can be reconstituted in *Nb*, although EDS1 proteins and functions have diverged between Arabidopsis and *Solanaceae* (Gantner *et al.*, 2018; Lapin *et al.*, 2019). Accordingly, induction of autoimmunity, at least in this case, is not predictive of immune functions of an incompatible allele. Similarly, activation of DM2h by old3-1 appears to depend on very specific properties of the incompatible allele (a point mutation); an *old3* loss-of-function T-DNA allele does not induce autoimmunity (Tahir *et al.*, 2013). Notably, also the activation of immune receptors involved in dominant HI can often be reconstituted in heterologous *Nb* assays, and is limited to very specific alleles of the non-NLR locus in populations (e.g., Chae *et al.*, 2014; Li *et al.*, 2020; Tran *et al.*, 2017). Therefore, we propose that autoimmunity in negative epistatic interactions involving NLRs may, at least in some cases, occur stochastically due to the recognition of corresponding patterns by NLRs. This shall function as a cautionary note for interpretation of dominant autoimmunity, in particular upon involvement of highly variable and thus risky NLRs.

EXPERIMENTAL PROCEDURES

Plant material and growth conditions

Nb plants were cultivated in a greenhouse with a 16-h light period (sunlight and/or IP65 lamps (Philips) equipped with Agro 400 W bulbs (SON-T); 130–150 μE m^{-2} sec; switchpoint; 100 μE m^{-2} sec), 60% relative humidity at 24/20°C (day/night). The *Nbeds1a-1* mutant line is published (Ordon *et al.*, 2017). Details on *Nbnrg1* mutant lines are provided in Figure S3. *Arabidopsis thaliana* plants were cultivated under short day conditions (8 h light, 23/21°C day/night, 60% relative humidity) or in a greenhouse under long day conditions (16 h light) for seed set. For suppression of autoimmunity, plants were germinated under short day conditions (7–8 days) and subsequently cultivated in a growth chamber with 28/26°C day/night temperatures and 12 h light (approximately 120 μE m^{-2} sec). For temperature-shift experiments, plants were moved into a growth chamber with 18/16°C day/night cycle (12 h illumination). For the induction of hybrid necrosis (*SRF3-DM2^{Ler}*), plants were grown with 14/12°C day/night temperatures under short day conditions for 4–6 weeks. Arabidopsis mutant or transgenic lines in the Col background (Col *eds1-2*, EDS1-YFP^{NLS}#A3 [in *eds1-2*], *dm2h^{nde1-1}* [in EDS1-YFP^{NLS}#A3], *np:DM2h* [in *dm2h^{nde1-1}*]) were previously described (Bartsch *et al.*, 2006; Stuttmann *et al.*, 2016). Mutant lines in the L*er* background used in this study were *eds1-2* (Aarts *et al.*, 1998), *rar1-13* (Muskett *et al.*, 2002) and several lines deficient in genes of the *DM2* cluster. DM2-deficient lines were reported previously (Ordon *et al.*, 2019; Ordon *et al.*, 2017) or details are provided in Figure S2. Furthermore, Arabidopsis accessions Kashmir and Kondara were used.

Sequencing of *nde1* alleles, *DM2h* cDNA cloning and multiple sequence alignments

DM2h was polymerase chain reaction (PCR)-amplified in two fragments using oligonucleotides JS724/1156 and JS1155/725 (Table S2). Amplicons were purified using a column-based kit and sequenced using oligonucleotides JS1153/729/731 and JS733/1381, respectively. To clone the *DM2h* cDNA, *DM2h* was first transiently expressed in *Nb* using a gDNA fragment under 35S promoter control. Tissues were used for RNA extraction at 2 dpi, and cDNA was generated using RevertAid Reverse Transcriptase (Thermo, www.thermofisher.com). *DM2h* was amplified from cDNA in five fragments to eliminate internal *BpiI* restrictions sites (domestication) during cloning, and to prune the second intron, which was retained in several fragments cloned from cDNA prepared from *Nb* (primers JS972/973, JS729/1035, JS1036/974,

JS975/976, JS977/978). Fragments were subcloned in pUC57 (cut/ligation with either *Sma*I or *Eco*RV), sequence-verified and combined in pICH41308 by a *Bpi*I cut/ligation reaction (Engler *et al.*, 2014). The final construct, pJOG273, was again verified by sequencing, and used as a template for all further clonings. Multiple sequence alignments were generated using T-Coffee (http://www.tcoffee.org/), and rendered using ESPript (http://espript.ibcp.fr; Robert and Gouet, 2014).

Infection assays and SA measurements

Infection assays with *Hpa* (isolates Emwa and Cala) were conducted as previously described (Stuttmann *et al.*, 2011). For infection assays with *Pst* DC3000, bacteria resuspended in 10 mM $MgCl_2$ were syringe-infiltrated into leaves of 4–6 week-old Arabidopsis plants at an OD_{600} = 0.0002. For day 0, samples were taken approximately 3 h after infiltration, and four replicates each consisting of three leaf discs were processed. On day 3, eight replicates were used. Leaf discs were shaken in 10 mM $MgCl_2$ containing 0.01% Silwet for 2–3 h, serial dilution series were prepared and plated for determination of colony forming units (cfu). For statistical analyses, data were normalized and/or transformed, and ANOVA with Tukey *post-hoc* test were used. Metabolite extractions for SA measurements were done essentially as described previously (Balcke *et al.*, 2017). Briefly, homogenized frozen material was cryo-extracted twice using 900 µl cold dichloromethane/ethanol and 150 µl aqueous hydrochloric acid buffer (pH 1.5). The organic phase was collected and the extraction residue was extracted again with tetrahydrofuran. Both extracts were combined and dried in a nitrogen stream. The dried residues were resuspended in 180 µl 80% methanol and centrifuged before injection. SA was measured using a Nucleoshell RP18 column (Macherey & Nagel, www.mn-net.com) on a Waters (www.waters.com) ACQUITY UPLC System (flow rate 400 µl min^{-1}, column temperature 40°C). Eluents A and B were aqueous 0.3 mmol L^{-1} NH4HCOO (adjusted to pH 3.5 with formic acid) and acetonitrile, respectively. Elution was performed as following: 0–2 min 5% eluent B, 2–19 min linear gradient to 95% B, 19–24 min 95% B. Mass spectrometric detection after electrospray ionization was performed via MS-TOF-SWATH-MS/MS (TripleToF 5600, both AB Sciex GmbH, https://sciex.com/) operating in negative ion mode and controlled by Analyst 1.6 TF software. Source operation parameters were as following: ion spray voltage, −4500 V; nebulizing gas, 60 psi; source temperature, 600°C; drying gas, 70 psi; curtain gas, 35 psi. SA was quantified using PeakView based on the [M–H] precursor *m*/*z* of 137.024 ± 0.02 Da and qualified via an authentic standard.

Transient protein expression, immunodetection and live cell imaging

Plate-grown bacteria (Agrobacterium strain GV3101 pMP90 or pMP90RK) were resuspended in Agro Infiltration Medium (10 mM MES pH 5.8, 10 mM $MgCl_2$) and infiltrated with a needless syringe at OD_{600} = 0.6 per strain. Cell death-based assays in *Nb* were repeated at least five times for evaluation of phenotypes, and detection of expressed fusion proteins was conducted for at least two replicates. For ultraviolet light documentation, *Nb* leaves were photographed on a gel documentation system (Alphalmager®) using a 5-sec exposure time (aperture 2.0). Image adjustments were applied to full images. Trypan blue staining was done as previously described (Stuttmann *et al.*, 2011). For incubation of *Nb* plants in the dark after infiltration, whole plants were placed in a growth cabinet (24/20°C, 16 h/8 h, 60% relative humidity) without illumination, and cell death was documented at 5 dpi. Samples for immunodetection of fusion proteins were taken at 3 dpi. Leaf discs were ground in liquid nitrogen, leaf powder resuspended in Laemmli buffer and proteins denatured by boiling. Total protein extracts were separated by sodium dodecyl sulfate–polyacrylamide gel electrophoresis and blotted onto nitrocellulose membranes. Primary antibodies were α-GFP (mouse) and α-hemagglutinin (rat; both from Roche), α-EDS1 (rabbit) and horseradish peroxidase-coupled (GE Healthcare) or alkaline phosphatase-coupled (Sigma-Aldrich, www.sigmaaldrich.com) secondary antibodies were used. A Zeiss LSM780 confocal laser scanning microscope was used for live cell imaging. All images are single planes.

Plant transformation and genome editing

Arabidopsis was transformed by floral dipping as previously described (Logemann *et al.*, 2006), and primary transformants were either selected by resistance to phosphinotricin (BASTA) or seed fluorescence (FAST; Shimada *et al.*, 2010). *Nb* was transformed as previously described (dx.doi.org/10.17504/protocols.io.; Gantner *et al.*, 2019), using previously described target sites/sgRNAs for *NRG1* editing (Qi *et al.*, 2018). Different versions of pDGE vectors (Barthel *et al.*, 2020; Ordon *et al.*, 2019; Ordon *et al.*, 2017) were used to generate *dm2* and *Nbnrg1* mutant lines by *Sp*Cas9. Respective target sites are provided in Figure S2 (Arabidopsis lines) and Figure S3 (*Nbnrg1*). sgRNAs were prepared by cloning of hybridized oligonucleotides in pDGE shuttle vectors, as previously described (Ordon *et al.*, 2017). Mutant lines were cured of the editing construct, with the exception of the *dm2-11* line.

Molecular cloning, genotyping and quantitative reverse transcription-PCR

The GoldenGate strategy (Engler *et al.*, 2008) was used for most clonings. Different DNA modules from the Modular Cloning system, the Plant Parts I and the Plant Parts II collections were used, and cut/ligation reactions employing either *Bsa*I or *Bpi*I together with T4 DNA Ligase (1–5 µ $µl^{-1}$; Thermo) were conducted using approximately 20 fmol of each DNA module as previously described (Engler *et al.*, 2014; Gantner *et al.*, 2018; Weber *et al.*, 2011). Additional plasmids were generated using Gateway cloning. In these cases, entry clones were generated by PCR (via TOPO cloning or GoldenGate cloning), and inserts were subsequently recombined into expression plasmids by LR reactions. Detailed information on plasmids used and/or generated in this study is provided in Table S3. A lab-internal Taq polymerase preparation was used for genotyping of different Arabidopsis lines. Genomic DNA was extracted by a CTAB protocol, and primer sequences are provided in Table S2. For transcript analyses, RNA was extracted by a TRIzol protocol, as previously described (Gantner *et al.*, 2019). The Reverse Transcriptase Core Kit was used for cDNA synthesis, and the Takyon No ROX SYBR 2× MasterMix Blue dTTP quantitative PCR Kit (both Eurogentec, www.eurogentec.com) for quantitative real-time PCR using a CFX96 detection system (Bio-Rad, www.bio-rad.com). Transcript data were normalized to *UBQ10*; primer sequences are provided in Table S2.

ACKNOWLEDGEMENTS

This work was funded by GRC grant STU 642-1/1 (Deutsche Forschungsgemeinschaft, DFG) to JS. UB is grateful for financial support by the Leibniz price from the DFG and the Alfried Krupp von Bohlen und Halbach Stiftung. FF was financed by an ERASMUS mobility program. We are grateful to Bianca Rosinsky for taking care of plant growth facilities and growing plants, and to Ruben Alcazar and Jane Parker for providing plasmids containing

SRF3^{Kond} or *RPP1-like R8/DM2h* genomic DNA fragments. Jan Kemna is acknowledged for cloning of the DM2h cDNA, and Samuel Grimm for primary screening of DM2h-YFP Arabidopsis transformants. Open Access funding enabled and organized by Projekt DEAL.

CONFLICT OF INTERESTS

The authors declare that they have no competing interests.

AUTHOR CONTRIBUTIONS

JO performed most experiments, analyzed data and drafted figures. PM, JE and FF performed additional experiments. GB performed SA measurements. JS designed the study, performed experiments, analyzed data, supervised experimental work and prepared final figures. JS and JO wrote the manuscript with contributions from JE. UB provided additional supervision and contributed to the final manuscript.

DATA AVAILABILITY STATEMENT

All relevant data supporting the findings of this work are available within the manuscript and the supporting materials.

SUPPORTING INFORMATION

Additional Supporting Information may be found in the online version of this article.

Figure S1. Sequence alignment of TIR and NB -ARC domains. Sequence alignment of TIR and NB -ARC domains.

Figure S2. *dm2* mutant lines used in this study.

Figure S3. Genotyping of hybrids obtained from crosses to accession Kondara.

Figure S4. A transient assay for reconstitution of DM2h activation in *N. benthamiana* based on protein co-expression and cell death induction.

Figure S5. Growth phenotype and immunoblot analysis of DM2h-YFP transgenic plants.

Figure S6. Molecular details on *Nbnrg1* mutant lines generated in this study.

Figure S7. Immunodetection and subcellular localization of EDS1-YFP^{NLS} variants differing in immune signaling competency.

Figure S8. Immunodetection and subcellular localization of EDS1-YFP^{NLS} variants differing in NLS and linker sequences.

Figure S9. CRISPR/Cas-induced *srf3* mutant alleles in accession L*er*.

Table S1. Molecular details on identified *dm2h/nde1* alleles.

Table S2. Oligonucleotides used in this study.

Table S3. Plasmids used in this study.

REFERENCES

Aarts, N., Metz, M., Holub, E., Staskawicz, B.J., Daniels, M.J. & Parker, J.E. (1998) Different requirements for *EDS1* and *NDR1* by disease resistance genes define at least two *R* gene-mediated signaling pathways in *Arabidopsis*. *Proceedings of the National Academy of Sciences of the United States of America*, **95**, 10306–10311.

Alcazar, R., Garcia, A.V., Kronholm, I., de Meaux, J., Koornneef, M., Parker, J.E. *et al.* (2010) Natural variation at Strubbelig Receptor Kinase 3 drives immune-triggered incompatibilities between *Arabidopsis thaliana* accessions. *Nature Genetics*, **42**, 1135–1139.

Alcazar, R., Garcia, A.V., Parker, J.E. & Reymond, M. (2009) Incremental steps toward incompatibility revealed by Arabidopsis epistatic interactions modulating salicylic acid pathway activation. *Proceedings of the National Academy of Sciences of the United States of America*, **106**, 334–339.

Alcazar, R. & Parker, J.E. (2011) The impact of temperature on balancing immune responsiveness and growth in Arabidopsis. *Trends in Plant Science*, **16**, 666–675.

Alcazar, R., von Reth, M., Bautor, J., Chae, E., Weigel, D., Koornneef, M. *et al.* (2014) Analysis of a plant complex resistance gene locus underlying immune-related hybrid incompatibility and its occurrence in nature. *PLoS Genetics*, **10**, e1004848.

Ariga, H., Katori, T., Tsuchimatsu, T., Hirase, T., Tajima, Y., Parker, J.E. *et al.* (2017) NLR locus-mediated trade-off between abiotic and biotic stress adaptation in Arabidopsis. *Nature Plants*, **3**, 17072.

Arora, D., Abel, N.B., Liu, C., Van Damme, P., Yperman, K., Eeckhout, D. *et al.* (2020) Establishment of proximity-dependent biotinylation approaches in different plant model systems. *The Plant Cell*, **32**, 3388–3407.

Atanasov, K.E., Liu, C., Erban, A., Kopka, J., Parker, J.E. & Alcazar, R. (2018) NLR mutations suppressing immune hybrid incompatibility and their effects on disease resistance. *Plant Physiology*, **177**, 1152–1169.

Balcke, G.U., Bennewitz, S., Bergau, N., Athmer, B., Henning, A., Majovsky, P. *et al.* (2017) Multi-omics of tomato glandular trichomes reveals distinct features of central carbon metabolism supporting high productivity of specialized metabolites. *The Plant Cell*, **29**, 960–983.

Barragan, C.A., Wu, R., Kim, S.T., Xi, W., Habring, A., Hagmann, J. *et al.* (2019) RPW8/HR repeats control NLR activation in *Arabidopsis thaliana*. *PLoS Genetics*, **15**, e1008313.

Barthel, K., Martin, P., Ordon, J., Erickson, J.L., Gantner, J., Herr, R. *et al.* (2020) One-shot generation of duodecuple (12x) mutant Arabidopsis: highly efficient routine editing in model species. *bioRxiv*, 2020.2003.2031.018671.

Bartsch, M., Gobbato, E., Bednarek, P., Debey, S., Schultze, J.L., Bautor, J. *et al.* (2006) Salicylic acid-independent ENHANCED DISEASE SUSCEPTIBILITY1 signaling in Arabidopsis immunity and cell death is regulated by the monooxygenase FMO1 and the Nudix hydrolase NUDT7. *The Plant Cell*, **18**, 1038–1051.

Bentham, A., Burdett, H., Anderson, P.A., Williams, S.J. & Kobe, B. (2017) Animal NLRs provide structural insights into plant NLR function. *Annals of Botany*, **119**, 689–702.

Bernoux, M., Burdett, H., Williams, S.J., Zhang, X., Chen, C., Newell, K. *et al.* (2016) Comparative analysis of the flax immune receptors L6 and L7 suggests an equilibrium-based switch activation model. *The Plant Cell*, **28**, 146–159.

Bhattacharjee, S., Halane, M.K., Kim, S.H. & Gassmann, W. (2011) Pathogen effectors target Arabidopsis EDS1 and alter its interactions with immune regulators. *Science*, **334**, 1405–1408.

Bomblies, K., Lempe, J., Epple, P., Warthmann, N., Lanz, C., Dangl, J.L. *et al.* (2007) Autoimmune response as a mechanism for a Dobzhansky-Muller-type incompatibility syndrome in plants. *PLoS Biology*, **5**, e236.

Bomblies, K. & Weigel, D. (2007) Hybrid necrosis: autoimmunity as a potential gene-flow barrier in plant species. *Nature Reviews Genetics*, **8**, 382–393.

Bonardi, V., Tang, S., Stallmann, A., Roberts, M., Cherkis, K. & Dangl, J.L. (2011) Expanded functions for a family of plant intracellular immune receptors beyond specific recognition of pathogen effectors. *Proceedings of the National Academy of Sciences of the United States of America*, **108**, 16463–16468.

Botella, M.A., Parker, J.E., Frost, L.N., Bittner-Eddy, P.D., Beynon, J.L., Daniels, M.J. *et al.* (1998) Three genes of the Arabidopsis RPP1 complex resistance locus recognize distinct Peronospora parasitica avirulence determinants. *The Plant cell*, **10**, 1847–1860.

Branon, T.C., Bosch, J.A., Sanchez, A.D., Udeshi, N.D., Svinkina, T., Carr, S.A. *et al.* (2018) Efficient proximity labeling in living cells and organisms with TurboID. *Nature Biotechnology*, **36**, 880–887.

Burch-Smith, T.M., Schiff, M., Caplan, J.L., Tsao, J., Czymmek, K. & Dinesh-Kumar, S.P. (2007) A novel role for the TIR domain in association with pathogen-derived elicitors. *PLoS Biology*, **5**, e68.

Burdett, H., Bentham, A.R., Williams, S.J., Dodds, P.N., Anderson, P.A., Banfield, M.J. *et al.* (2019) The plant "resistosome": structural insights into immune signaling. *Cell Host & Microbe*, **26**, 193–201.

Castel, B., Ngou, P.M., Cevik, V., Redkar, A., Kim, D.S., Yang, Y. *et al.* (2019) Diverse NLR immune receptors activate defence via the RPW8-NLR NRG1. *New Phytologist*, **222**, 966–980.

Chae, E., Bomblies, K., Kim, S.T., Karelina, D., Zaidem, M., Ossowski, S. *et al.* (2014) Species-wide genetic incompatibility analysis identifies immune genes as hot spots of deleterious epistasis. *Cell*, **159**, 1341–1351.

Chakraborty, J., Ghosh, P. & Das, S. (2018) Autoimmunity in plants. *Planta*, **248**, 751–767.

Chou, S., Krasileva, K.V., Holton, J.M., Steinbrenner, A.D., Alber, T. & Staskawicz, B.J. (2011) Hyaloperonospora arabidopsidis ATR1 effector is a repeat protein with distributed recognition surfaces. *Proceedings of the National Academy of Sciences of the United States of America*, **108**, 13323–13328.

Collier, S.M., Hamel, L.P. & Moffett, P. (2011) Cell death mediated by the N-terminal domains of a unique and highly conserved class of NB-LRR protein. *Molecular Plant-Microbe Interactions*, **24**, 918–931.

Cui, H., Tsuda, K. & Parker, J.E. (2015) Effector-triggered immunity: from pathogen perception to robust defense. *Annual Review of Plant Biology*, **66**, 487–511.

Dodds, P.N. & Rathjen, J.P. (2010) Plant immunity: towards an integrated view of plant-pathogen interactions. *Nature Reviews Genetics*, **11**, 539–548.

Duxbury, Z., Wang, S., MacKenzie, C.I., Tenthorey, J.L., Zhang, X., Huh, S.U. *et al.* (2020) Induced proximity of a TIR signaling domain on a plant-mammalian NLR chimera activates defense in plants. *Proceedings of the National Academy of Sciences of the United States of America*, **117**, 18832–18839.

Engler, C., Kandzia, R. & Marillonnet, S. (2008) A one pot, one step, precision cloning method with high throughput capability. *PLoS ONE*, **3**, e3647.

Engler, C., Youles, M., Gruetzner, R., Ehnert, T.M., Werner, S., Jones, J.D., *et al.* (2014) A golden gate modular cloning toolbox for plants. *ACS Synthetic Biology*, **3**(11), 839–843.

Gantner, J., Ordon, J., Ilse, T., Kretschmer, C., Gruetzner, R., Lofke, C. *et al.* (2018) Peripheral infrastructure vectors and an extended set of plant parts for the Modular Cloning system. *PLoS ONE*, **13**, e0197185.

Gantner, J., Ordon, J., Kretschmer, C., Guerois, R. & Stuttmann, J. (2019) An EDS1-SAG101 complex is essential for TNL-mediated immunity in *Nicotiana benthamiana*. *The Plant Cell*, **31**, 2456–2474.

Goritschnig, S., Steinbrenner, A.D., Grunwald, D.J. & Staskawicz, B.J. (2016) Structurally distinct Arabidopsis thaliana NLR immune receptors recognize tandem WY domains of an oomycete effector. *New Phytologist*, **210**, 984–996.

Holub, E.B., Beynon, J.L. & Crute, I.R. (1994) Phenotypic and genotypic characterization of interactions between isolates of *Peronospora parasitica* and accessions of *Arabidopsis thaliana*. *Molecular Plant-Microbe Interactions*, **7**, 223–239.

Horsefield, S., Burdett, H., Zhang, X.X., Manik, M.K., Shi, Y., Chen, J. *et al.* (2019) NAD(+) cleavage activity by animal and plant TIR domains in cell death pathways. *Science*, **365**, 793.

Huh, S.U., Cevik, V., Ding, P., Duxbury, Z., Ma, Y., Tomlinson, L. *et al.* (2017) Protein-protein interactions in the RPS4/RRS1 immune receptor complex. *PLoS Pathogens*, **13**, e1006376.

Jacob, F., Vernaldi, S. & Maekawa, T. (2013) Evolution and conservation of plant NLR functions. *Frontiers in Immunology*, **4**, 297.

Jiao, W.B. & Schneeberger, K. (2020) Chromosome-level assemblies of multiple Arabidopsis genomes reveal hotspots of rearrangements with altered evolutionary dynamics. *Nature Communications*, **11**, 989.

Jones, J.D. & Dangl, J.L. (2006) The plant immune system. *Nature*, **444**, 323–329.

Jubic, L.M., Saile, S., Furzer, O.J., El Kasmi, F. & Dangl, J.L. (2019) Help wanted: helper NLRs and plant immune responses. *Current Opinion in Plant Biology*, **50**, 82–94.

Kim, S.H., Gao, F., Bhattacharjee, S., Adiasor, J.A., Nam, J.C. & Gassmann, W. (2010) The Arabidopsis resistance-like gene SNC1 is activated by mutations in srfr1 and contributes to resistance to the bacterial effector AvrRps4. *PLoS Pathogens*, **6**(11), e1001172.

Kim, W., Latrasse, D., Servet, C. & Zhou, D.X. (2013) Arabidopsis histone deacetylase HDA9 regulates flowering time through repression of AGL19. *Biochemical and Biophysical Research Communications*, **432**, 394–398.

Kourelis, J. & van der Hoorn, R.A.L. (2018) Defended to the nines: 25 years of resistance gene cloning identifies nine mechanisms for R protein function. *The Plant Cell*, **30**, 285–299.

Krasileva, K.V., Dahlbeck, D. & Staskawicz, B.J. (2010) Activation of an Arabidopsis resistance protein is specified by the in planta association of its leucine-rich repeat domain with the cognate oomycete effector. *The Plant Cell*, **22**, 2444–2458.

Laflamme, B., Dillon, M.M., Martel, A., Almeida, R.N.D., Desveaux, D. & Guttman, D.S. (2020) The pan-genome effector-triggered immunity landscape of a host-pathogen interaction. *Science*, **367**, 763–768.

Lapin, D., Kovacova, V., Sun, X., Dongus, J.A., Bhandari, D.D., von Born, P. *et al.* (2019) A coevolved EDS1-SAG101-NRG1 module mediates cell death signaling by TIR-domain immune receptors. *The Plant Cell*, **31**, 2430–2455.

Lee, R.R.Q. & Chae, E. (2020) Variation patterns of NLR clusters in *Arabidopsis thaliana* genomes. *Plant Communications*, **1**(4), 100089.

Li, L., Habring, A., Wang, K. & Weigel, D. (2020) Atypical resistance protein RPW8/HR triggers oligomerization of the NLR immune receptor RPP7 and autoimmunity. *Cell Host & Microbe*, **27**(3), 405–417.e6.

Li, X., Clarke, J.D., Zhang, Y. & Dong, X. (2001) Activation of an EDS1-mediated R-gene pathway in the snc1 mutant leads to constitutive, NPR1-independent pathogen resistance. *Molecular Plant-Microbe Interactions*, **14**, 1131–1139.

Logemann, E., Birkenbihl, R.P., Ulker, B. & Somssich, I.E. (2006) An improved method for preparing Agrobacterium cells that simplifies the Arabidopsis transformation protocol. *Plant Methods*, **2**, 16.

Luker, K.E., Smith, M.C., Luker, G.D., Gammon, S.T., Piwnica-Worms, H. & Piwnica-Worms, D. (2004) Kinetics of regulated protein-protein interactions revealed with firefly luciferase complementation imaging in cells and living animals. *Proceedings of the National Academy of Sciences of the United States of America*, **101**, 12288–12293.

Ma, S., Lapin, D., Liu, L., Sun, Y., Song, W., Zhang, X. *et al.* (2020) Direct pathogen-induced assembly of an NLR immune receptor complex to form a holoenzyme. *Science*, **370**.

Mair, A., Xu, S.L., Branon, T.C., Ting, A.Y. & Bergmann, D.C. (2019) Proximity labeling of protein complexes and cell-type-specific organellar proteomes in Arabidopsis enabled by TurboID. *eLife*, **8**.

Martin, E.C., Sukarta, O.C.A., Spiridon, L., Grigore, L.G., Constantinescu, V., Tacutu, R. *et al.* (2020a) LRRpredictor – a new LRR motif detection method for irregular motifs of plant NLR proteins using an ensemble of classifiers. *Genes*, **11**(3), 286.

Martin, R., Qi, T., Zhang, H., Liu, F., King, M., Toth, C. *et al.* (2020b) Structure of the activated ROQ1 resistosome directly recognizing the pathogen effector XopQ. *Science*, **370**, eabd9993.

Meyers, B.C., Kozik, A., Griego, A., Kuang, H. & Michelmore, R.W. (2003) Genome-wide analysis of NBS-LRR-encoding genes in Arabidopsis. *The Plant Cell*, **15**, 809–834.

Muskett, P.R., Kahn, K., Austin, M.J., Moisan, L.J., Sadanandom, A., Shirasu, K. *et al.* (2002) Arabidopsis *RAR1* exerts rate-limiting control of *R* gene- mediated defenses against multiple pathogens. *The Plant Cell*, **14**, 979–992.

Ngou, B.P.M., Ahn, H.-K., Ding, P. & Jones, J.D. (2020) Mutual potentiation of plant immunity by cell-surface and intracellular receptors. *bioRxiv*, 2020.2004.2010.034173.

Noël, L., Moores, T.L., van der Biezen, E.A., Parniske, M., Daniels, M.J., Parker, J.E. *et al.* (1999) Pronounced intraspecific haplotype divergence at the RPP5 complex disease resistance locus of Arabidopsis. *The Pant Cell*, **11**, 2099–2111.

Ordon, J., Bressan, M., Kretschmer, C., Dall'Osto, L., Marillonnet, S., Bassi, R. *et al.* (2020) Optimized Cas9 expression systems for highly efficient Arabidopsis genome editing facilitate isolation of complex alleles in a single generation. *Functional & Integrative Genomics*, **20**(1), 151–162.

Ordon, J., Gantner, J., Kemna, J., Schwalgun, L., Reschke, M., Streubel, J. *et al.* (2017) Generation of chromosomal deletions in dicotyledonous plants employing a user-friendly genome editing toolkit. *The Plant Journal*, **89**, 155–168.

Park, H.J., Baek, D., Cha, J.Y., Liao, X., Kang, S.H., McClung, C.R. *et al.* (2019) HOS15 interacts with the histone deacetylase HDA9 and the evening complex to epigenetically regulate the floral activator GIGANTEA. *The Plant Cell*, **31**, 37–51.

Parker, J.E., Coleman, M.J., Szabo, V., Frost, L.N., Schmidt, R., van der Biezen, E.A. *et al.* (1997) The Arabidopsis downy mildew resistance gene

RPP5 shares similarity to the toll and interleukin-1 receptors with N and L6. *The Plant Cell*, **9**, 879–894.

Prigozhin, D.M. & Krasileva, K.V. (2021) Analysis of intraspecies diversity reveals a subset of highly variable plant immune receptors and predicts their binding sites. *The Plant Cell*. https://doi.org/10.1093/plcell/koab013.

Qi, D., DeYoung, B.J. & Innes, R.W. (2012) Structure-function analysis of the coiled-coil and leucine-rich repeat domains of the RPS5 disease resistance protein. *Plant Physiology*, **158**, 1819–1832.

Qi, T., Seong, K., Thomazella, D.P.T., Kim, J.R., Pham, J., Seo, E. *et al.* (2018) NRG1 functions downstream of EDS1 to regulate TIR-NLR-mediated plant immunity in *Nicotiana benthamiana*. *Proceedings of the National Academy of Sciences of the United States of America*, **115**, E10979–E10987.

Rehmany, A.P., Gordon, A., Rose, L.E., Allen, R.L., Armstrong, M.R., Whisson, S.C. *et al.* (2005) Differential recognition of highly divergent downy mildew avirulence gene alleles by RPP1 resistance genes from two Arabidopsis lines. *The Plant Cell*, **17**, 1839–1850.

Robert, X. & Gouet, P. (2014) Deciphering key features in protein structures with the new ENDscript server. *Nucleic Acids Research*, **42**, W320–W324.

Rodriguez, E., El Ghoul, H., Mundy, J. & Petersen, M. (2016) Making sense of plant autoimmunity and 'negative regulators'. *FEBS Journal*, **283**, 1385–1391.

Saijo, Y., Loo, E.P. & Yasuda, S. (2018) Pattern recognition receptors and signaling in plant-microbe interactions. *The Plant Journal*, **93**, 592–613.

Saile, S.C., Jacob, P., Castel, B., Jubic, L.M., Salas-Gonzales, I., Backer, M. *et al.* (2020) Two unequally redundant "helper" immune receptor families mediate Arabidopsis thaliana intracellular "sensor" immune receptor functions. *PLoS Biology*, **18**, e3000783.

Saur, I.M., Bauer, S., Kracher, B., Lu, X., Franzeskakis, L., Muller, M.C. *et al.* (2019) Multiple pairs of allelic MLA immune receptor-powdery mildew AVRA effectors argue for a direct recognition mechanism. *eLife*, **8**.

Schneeberger, K., Ossowski, S., Lanz, C., Juul, T., Petersen, A.H., Nielsen, K.L. *et al.* (2009) SHOREmap: simultaneous mapping and mutation identification by deep sequencing. *Nature Methods*, **6**, 550–551.

Schreiber, K.J., Bentham, A., Williams, S.J., Kobe, B. & Staskawicz, B.J. (2016) Multiple domain associations within the Arabidopsis immune receptor RPP1 regulate the activation of programmed cell death. *PLoS Pathogens*, **12**, e1005769.

Shimada, T.L., Shimada, T. & Hara-Nishimura, I. (2010) A rapid and non-destructive screenable marker, FAST, for identifying transformed seeds of *Arabidopsis thaliana*. *The Plant Journal*, **61**, 519–528.

Sinapidou, E., Williams, K., Nott, L., Bahkt, S., Tor, M., Crute, I. *et al.* (2004) Two TIR:NB:LRR genes are required to specify resistance to Peronospora parasitica isolate Cala2 in Arabidopsis. *The Plant Journal*, **38**, 898–909.

Song, W., Forderer, A., Yu, D. & Chai, J. (2020) Structural biology of plant defence. *New Phytologist*, **229**(2), 692–711.

Steinbrenner, A.D., Goritschnig, S. & Staskawicz, B.J. (2015) Recognition and activation domains contribute to allele-specific responses of an Arabidopsis NLR receptor to an oomycete effector protein. *PLoS Pathogens*, **11**, e1004665.

Stuttmann, J., Hubberten, H.M., Rietz, S., Kaur, J., Muskett, P., Guerois, R. *et al.* (2011) Perturbation of Arabidopsis amino acid metabolism causes incompatibility with the adapted biotrophic pathogen Hyaloperonospora arabidopsidis. *The Plant cell*, **23**, 2788–2803.

Stuttmann, J., Peine, N., Garcia, A.V., Wagner, C., Choudhury, S.R., Wang, Y. *et al.* (2016) *Arabidopsis thaliana* DM2h (R8) within the Landsberg RPP1-like resistance locus underlies three different cases of EDS1-conditioned autoimmunity. *PLoS Genetics*, **12**, e1005990.

Tahir, J., Watanabe, M., Jing, H.C., Hunter, D.A., Tohge, T., Nunes-Nesi, A. *et al.* (2013) Activation of R-mediated innate immunity and disease susceptibility is affected by mutations in a cytosolic O-acetylserine (thiol) lyase in Arabidopsis. *The Plant Journal*, **73**, 118–130.

Tran, D.T.N., Chung, E.H., Habring-Muller, A., Demar, M., Schwab, R., Dangl, J.L. *et al.* (2017) Activation of a plant NLR complex through heteromeric association with an autoimmune risk variant of another NLR. *Current Biology*, **27**, 1148–1160.

van Wersch, R., Li, X. & Zhang, Y. (2016) Mighty dwarfs: Arabidopsis Autoimmune mutants and their usages in genetic dissection of plant immunity. *Frontiers in Plant Science*, **7**, 1717.

van Wersch, S. & Li, X. (2019) stronger when together: clustering of plant NLR Disease Resistance Genes. *Trends in Plant Science*, **24**, 688–699.

Wagner, S., Stuttmann, J., Rietz, S., Guerois, R., Brunstein, E., Bautor, J. *et al.* (2013) Structural basis for signaling by exclusive EDS1 heteromeric complexes with SAG101 or PAD4 in plant innate immunity. *Cell Host & Microbe*, **14**, 619–630.

Wan, L., Essuman, K., Anderson, R.G., Sasaki, Y., Monteiro, F., Chung, E.H. *et al.* (2019) TIR domains of plant immune receptors are NAD(+)-cleaving enzymes that promote cell death. *Science*, **365**, 799–803.

Wang, J., Hu, M., Wang, J., Qi, J., Han, Z., Wang, G. *et al.* (2019a) Reconstitution and structure of a plant NLR resistosome conferring immunity. *Science*, **364**, eaav5870.

Wang, J., Wang, J., Hu, M., Wu, S., Qi, J., Wang, G. *et al.* (2019b) Ligand-triggered allosteric ADP release primes a plant NLR complex. *Science*, **364**, eaav5868.

Weber, E., Engler, C., Gruetzner, R., Werner, S. & Marillonnet, S. (2011) A modular cloning system for standardized assembly of multigene constructs. *PLoS ONE*, **6**, e16765.

Van de Weyer, A.-L., Monteiro, F., Furzer, O.J., Nishimura, M.T., Cevik V., Witek, K. *et al.* (2019) A species-wide inventory of NLR genes and alleles in *Arabidopsis thaliana*. *Cell*, **178**(5), 1260–1272.e14.

Williams, S.J., Sohn, K.H., Wan, L., Bernoux, M., Sarris, P.F., Segonzac, C. *et al.* (2014) Structural basis for assembly and function of a heterodimeric plant immune receptor. *Science*, **344**, 299–303.

Wirthmueller, L., Zhang, Y., Jones, J.D. & Parker, J.E. (2007) Nuclear accumulation of the Arabidopsis immune receptor RPS4 is necessary for triggering EDS1-dependent defense. *Current Biology*, **17**, 2023–2029.

Wu, Z., Li, M., Dong, O.X., Xia, S., Liang, W., Bao, Y. *et al.* (2018) Differential regulation of TNL-mediated immune signaling by redundant helper CNLs. *New Phytologist*, **222**(2), 938–953.

Xu, F., Kapos, P., Cheng, Y.T., Li, M., Zhang, Y. & Li, X. (2014) NLR-associating transcription factor bHLH84 and its paralogs function redundantly in plant immunity. *PLoS Pathogens*, **10**, e1004312.

Yang, L., Chen, X., Wang, Z., Sun, Q., Hong, A., Zhang, A. *et al.* (2020) HOS15 and HDA9 negatively regulate immunity through histone deacetylation of intracellular immune receptor NLR genes in Arabidopsis. *New Phytologist*, **226**, 507–522.

Yuan, M., Jiang, Z., Bi, G., Nomura, K., Liu, M., He, S.Y., *et al.* Pattern-recognition receptors are required for NLR-mediated plant immunity. *bioRxiv*, 2020.2004.2010.031294.

Zhang, X., Bernoux, M., Bentham, A.R., Newman, T.E., Ve, T., Casey, L.W. *et al.* (2017) Multiple functional self-association interfaces in plant TIR domains. *Proceedings of the National Academy of Sciences of the United States of America*, **114**, E2046–E2052.